DEFINING THE FLOW FIELD OF AN OPEN-JET WIND TUNNEL

By

Donald B. Poole and Duane E. Cromack

Contract No. ONR-N00014-68-A-0146-12
Report No. THEMIS-UM-70-3

DISTRIBUTION OF THIS DOCUMENT IS UNLIMITED

Approved for Release

Reproduction in whole or in part is permitted for any purpose of the United States Government. This research was sponsored by the Office of Naval Research under ONR Contract No. N00014-68-A-0146, Subcontract No. N00014-68-A-0146-12, ONR Contract Authority Identification No. NR 200-016.

Charles E. Hutchinson
Co-Manager, Project THEMIS
University of Massachusetts

ABSTRACT

This investigation deals with mapping the velocities at successive cross-sectional planes in the test section of an open-jet wind tunnel. The instrumentation was chosen so that the total uncertainty on the calculated velocity would be less than 1% with a 95% confidence level.

The jet was studied using photography and a grid-and-tuft scheme, and it was determined that the same flow characteristics appear at both high and low flow rates.

The best probable location for model testing was determined to be $1\frac{1}{4}$ ft. to $2\frac{1}{2}$ ft. away from the exit plane of the tunnel as indicated by the combined pressure measurements and the photographic studies. It was also noted that turbulent mixing occurred between the jet and the still air in the room. The turbulence had a tendency to move in toward the center of the jet at successive planes from the exit plane of the tunnel. The most drastic change in turbulent mixing occurred at a cross section 3 ft. away from the exit plane. Recommendations for alterations to the facility are made for testing at or near the 3 ft. location.

ACKNOWLEDGMENT

This research was accomplished with the support of the Office of Naval Research. Appreciation is expressed to Dr. G. Albert Russell for his consultation and to Mrs. Nancy S. Poole for typing this report. Gratitude is also expressed for the photographic work provided by the University of Massachusetts Photo Center.

LIST OF FIGURES

LIST OF TABLES

TABLE OF CONTENTS

I. INTRODUCTION

This investigation deals with defining the low-speed flow field in terms of mapping the velocity profiles at successive cross sections in the test section of the Themis open-jet wind tunnel.

This tunnel was designed and constructed under the current Themis grant. Fig. 1 shows a side view of this tunnel with dimensions. Central to the design is a Buffalo Forge, Type S, Adjustax Vaneaxial Fan, which is driven by a 75 HP. A.C. electric motor. By adjusting fan blade vane angles, changing belt pulley diameters and varying the inlet damper settings, an approximate range of 10,000 to 68,000 CFM may be obtained.

Figs. 2 and 3 show the fan, wind tunnel and test section. It can be seen from Fig. 2 that the wind tunnel exhausts into the open room and then out through the wall, hence the term open-jet. The advantage of an open-jet wind tunnel is that it has a uniform constant pressure boundary, which does away with boundary layer effects encountered in a closed test section tunnel. The constant pressure boundary in this case is the atmospheric pressure of the room.

It is expected that when an open-jet discharges into a room, the stream diverges slightly on all sides, and mixing or turbulence occurs at the boundaries of the stream. The exit dimensions of the wind tunnel are 4 ft. x 4 ft. and these dimensions describe the maximum outer edges of the test section. It is conventional to assume that the test section extends away from the exit plane one exit plane diameter. In this case, one diameter would be 4 ft. providing a maximum testing region of 4 ft. x 4 ft. x 4 ft.

An open-jet flow field is totally defined when the distribution of static, dynamic and total pressures plus the distribution of temperature and turbulence are known.[1] Therefore when testing the characteristics of an air stream, the problem becomes basically an instrumentation problem.

The parameters to be measured are dynamic, static and total pressure, and a temperature in the air stream. These parameters will later be used to calculate velocities. It is necessary for an experimenter to ascertain an accurate final result with a predetermined uncertainty level. Therefore, when the parameters being measured during the experimentation are taken, the experimenter must know how accurately to measure each one. Once the uncertainty of the result, at a certain confidence level, is decided upon it then becomes necessary to choose the instrumentation which will produce this desired result. For this investigation it was desirous to calculate velocity with a total uncertainty at each point to be less than 1% with (20:1) odds. From an investigation of the theory of measurements,[3,4,5] it can be seen that the use of an instrument or meter, and the confidence level placed on the measurements taken in a single sample, are left to the discretion and experience of the user. A confidence level of (20:1) was postulated for velocity and by an investigation of manufacturers' literature,[6] Power Test Codes,[3,4] and consultation with more experienced experimenters; an uncertainty, at the confidence level of (20:1), was arrived at for each measurement to be taken.

By using a procedure outlined in "Describing Uncertainties in Single-Sample Experiments"[2] by Kline and McClintock, it is then possible

to calculate the velocity and its uncertainty, knowing the values of and uncertainties on the measurements taken of static, dynamic and total pressure and an air stream temperature. The Kline and McClintock procedure was used to "size" the instruments to the parameters to be measured and to calculate velocities and uncertainties at a specified confidence level in this investigation.

II. JUSTIFICATION

The justification for conducting this investigation is to define the outer boundaries of the open-jet and to map the velocities in the core of this jet. The data obtained during such an investigation is pertinent for two main reasons:

1. The flow characteristics must be examined to see if the fan and wind tunnel are performing as predescribed by the design specifications; and if not, to change the flow characteristics.
2. To provide a set of data on the velocity and pressure distributions for any experimenter who may choose to do test work with models.

III. PLAN OF WORK

It is proposed to conduct an investigation of the low-speed air stream in the test section of the Themis open-jet wind tunnel. A low-speed air stream is defined with respect to velocity, when the distributions of dynamic pressure, static pressure and temperature are known.[1]

It is proposed to determine the distributions of dynamic, static and total pressure; and to measure a temperature of the air stream for the following two flow rates: (20,000 and 60,000 CFM).

It is further proposed to examine the flow visually by photographic techniques using a grid-and-tuft device[1] in an attempt to visually define the boundary dimensions of the flow core and to examine the steadiness of flow in successive cross sections in the test section.

IV. EXPERIMENTAL APPARATUS AND PROCEDURE

A. Instrumentation

The instrumentation used in the measurement of the pressure parameters and air stream temperature were as follows:

Parameter	-	Instrument
Static and Total Pressure	-	$\frac{1}{4}$ in. diameter Pitot tube 6 in. x 24 in. long
Dynamic Pressure	-	Flow Corporation, Model MM3, Micromanometer
		Resolution: $\pm$ 0.0001 in. of Manometer fluid
		Accuracy: $\pm$ 0.0002 in. of Manometer fluid
		Manometer fluid - Butyl alcohol
		Maximum Pressure Difference - 2 in. of Manometer fluid
Air Stream Temperature	-	Artco - 38017 P Glass Lab-Type Thermometer
		Scale: 0 - 220°F in 2° increments
Static Pressure	-	Manning, Maxwell and Moore - Naval Type - Mercury barometer. Charts for temperature and latitude corrections were available.
Time	-	Standard 0 - 15 min. stop watch

B. Apparatus

Photographs of the wind tunnel and fan used in this investigation can be seen in Figs. 1, 2 and 3. Fig. 1 shows a side view of the wind tunnel with dimensions. It can be seen from this figure that the tunnel is constructed in three sections. A diverging inlet section, a plenum chamber complete with perforated plates, one layer of honeycomb

and several fine mesh screens, and a convergent section with an exit area of 4 square feet.

Air is supplied to the tunnel by a Buffalo Forge, Type S, Adjustax Vaneaxial Fan. The fan has 10 adjustable angle blades and an adjustable, manually operated, inlet damper so that the volume flow rate may be varied. The fan is powered by a 75 HP. A.C. electric motor turning a multi-sheaved V-belt pulley. By varying pulley diameters, blade angles and inlet damper settings, a range of flow rates between 10,000 to 68,000 CFM can be achieved.

The apparatus used for locating the pitot tube in the test section can be seen in Fig. 4. This apparatus consists of a test stand constructed of 9 in. channel iron, held approximately 2 ft. - 8 in. above the floor by standard-size cement blocks. Secured tightly to the upper side of the channel iron are a series of 3/4 in. diameter pipes. The pipes are spaced so that they form reference locations for each successive cross-sectional plane moving away from the exit plane of the wind tunnel. The spacings were: 6 in. from the exit plane, and then at every 18 in. for 4 spaces.

A reference frame was constructed from 3/4 in. square stock with base dimensions of 3 ft. - 6 in. long by 2 ft. - 6 in. wide. A 5 ft. tall mast was erected on the base and braced with a piece of 1/2 in. diameter pipe. The reference frame was then placed on top of the test stand with the bottom leading edge resting against the first 3/4 in. diameter pipe.

A grid-and-tuft system, shown in Fig. 16, was constructed so that the flow could be examined visually. It consisted of a 2 x 4 in. wooden

support frame with a 6 ft. square grid area. The grid was constructed by stringing 0.20 in. diameter piano wire across the frame at 4 in. spacings both in the vertical and horizontal directions and then stapling the wire down with poultry staples. The support frame resembled that of a portable blackboard frame, with the center line of the grid at the same height as the center line of the air stream. Tufts of 3/4 ounce baby yarn, 8-3/4 in. long were tied to the intersection of each square of the grid.

C. Procedure

a. Preliminary Procedure for Pressure Measurements

After the test stand and reference frame were positioned and leveled, the center line of the exit plane was determined. This was accomplished by running two pieces of string diagonally across to opposite corners of the wind tunnel exit. A 5 ft. length of tape measure was cemented to the front side of the mast of the reference frame with a convenient inch mark being placed directly opposite the point where the strings crossed. The pitot tube was clamped to the mast over the tape measure. With the reference frame still located at the center line of the exit, lines were scribed on the pipes, on either side of the reference frame, at 4 in. spacing for the width of the test stand. Thus by moving the pitot tube vertically or sliding the reference frame horizontally any point in the exit plane could be located accurately to within $\pm$ 1/8 in. Mapping of successive cross-sectional planes was achieved by moving the reference frame back on the test stand the desired number of spacings between pipes.

The pitot tube was connected to the micromanometer by two 15 ft.

lengths of $\frac{1}{4}$ in. Tygon tubing. The micromanometer was set off to one side of the air stream, and it became necessary to counterweight the Tygon tubing so that it would not dangle in the air stream. This was accomplished by attaching a piece of string to each piece of tubing, and then passing the string through a lifting lug on the top of the wind tunnel. A 1 in. diameter pipe coupling was tied to the end of each string and then allowed to hang over the edge of the wind tunnel. As the reference frame and pitot tube were moved the weight of the pipe couplings took up any slack in the tubing.

b. Testing Procedure for Pressure Measurements

Before testing started, it was noted that the fan blade angles were set near their maximum position and that the larger of the two pulleys was installed on the drive motor. It was therefore decided that testing would initially be undertaken at a high flow rate of approximately 66,000 CFM. An inlet damper setting was found which produced this flow and a mark was then scribed on the damper adjusting mechanism so that the same setting could be achieved at any desired time.

The micromanometer was placed on a table off to the side of the test section. The Tygon tubing from the pitot tube was then attached to the inlet connections of the micromanometer. The wind tunnel was started up and allowed to run for approximately 20 minutes; letting the temperature in the room come to equilibrium. After equilibrium was reached, the mercury barometer and attached thermometer were read and the readings corrected for temperature and latitude.

At this point a digression will be made to explain the principles

and operation of the micromanometer. This instrument operates on the nulling principles first proposed by Prandtl. Two unknown pressures are brought to bear on either side of a U-tube. The U-tube in this case, having a large reservoir as one leg and a $\frac{1}{4}$ in. diameter sloping glass tube as the other. To use, the operator adjusts the height of the glass tube until the meniscus is restored exactly to the position it occupied before the unknown pressures were applied. The meniscus is observed through a magnifying eye piece relative to a fixed hair-line, and the vertical displacement of the tube required to restore the meniscus to its known position is read with a vernier micrometer calibrated directly in 0.0001 in. increments.

The micromanometer also comes equipped with a thermometer so that the Butyl alcohol in the reservoir can be corrected for thermal expansion due to any ambient temperature changes.

The reference or zero reading is obtained by applying equal pressure to each leg of the U-tube. This is done by turning one of the taps, to which one of the unknown pressures is connected, to its zero position. After the zero reading is recorded, the tap is turned back to its "on" position and the pressure readings may be obtained. The absolute pressure difference is then equal to the reading obtained minus the zero reading.

With the fan running, the zero reading in the manometer was recorded. This reading usually did not change during a day's testing, but did change from one day to the next. This is due to the thermal expansion effects on the $\frac{1}{2}$ pint of Butyl alcohol in the reservoir.

The air stream temperature was obtained by hanging a glass

lab-type thermometer in the jet. The thermometer was attached to the clamp holding the pitot tube to the mast. The thermometer was hung in position before the wind tunnel was started so that the time used to equalize room conditions upon start up was also used to allow the thermometer to reach an equilibrium.

By moving the reference frame and pitot tube as prescribed in the apparatus section, pressure measurements were taken at the points indicated in Fig. 5. Ten readings of dynamic pressure were taken at each point indicated on the figure. This procedure was followed for measurements in the exit plane twice. Once with the tunnel in the original location, and then with the tunnel raised 2-3/4 in. Measurements were also taken at a plane 1-1/2 ft. away from the exit plane.

The barometric pressure, air stream temperature and Butyl alcohol reservoir temperature were observed several times during the course of a day's testing, and the arithmetic average used in calculations.

c. Procedure for Photographic Study in Air Stream

A photographic study was undertaken to observe the air stream flow visually. This was done for a relatively high volume flow rate and a relatively low flow rate. The camera was set up on a tripod approximately 10 ft. away from the exit plane of the wind tunnel. The tripod was then raised until the center line of the exit plane coincided with the center line of the camera lens. The grid-and-tuft network was then set at the exit plane of the wind tunnel; allowing equal distance between the edge of the wooden support frame and discharge on all sides. Light meter readings were taken and the exposure of the film set. It was decided to use time-elapse photography since it was motions of the yarn tufts that

was sought. Any such motions would create a slight blur in the photograph at the particular tuft and therefore make itself distinguishable. The maximum exposure setting of 1 second was used for all photographs taken during this study.

The wind tunnel was turned on and allowed to run for approximately 20 minutes. A photograph was then taken at the exit plane at the near-open damper setting. The damper was then closed to its $\frac{1}{4}$ open position (approximately) and another photograph taken at the exit plane. While the damper was at the near-closed position, a line was scribed on the mechanism so that the same location could be obtained again.

The grid-and-tuft system was then moved in succession from the exit plane to the locations of $1\frac{1}{2}$ ft., 3 ft., and 4 ft. away from the exit plane. Two photographs were taken at each location. One each for high and low flow rates. It became necessary at the 4 ft. location to switch the camera lens to a wide optical lens, thus allowing approximately the same grid area to be photographed throughout the study.

d. Procedure for Conducting Circulation Study

A circulation study was undertaken in the room. This was done with a polaroid camera and tufted grid and later with a cloud maker. The grid-and-tuft scheme was photographed at different locations in the room occupied by the wind tunnel. The first photograph was taken with the grid-and-tuft system placed in the double doorway that entered the room from the left side. Fig. 2 shows the location of this entrance, to the room. The grid system was then rotated 90° clockwise and moved toward the front wall approximately 3 ft. This was done to try and

distinguish, in a quantitative way, how much flow was recirculating from the open-jet and how much was being drawn in from the side room. A photograph was taken at this location, and the grid-and-tuft system then moved to the right side of the wind tunnel. The grid system was then located at approximately the same location along the side of the tunnel and a photograph taken. It was hoped that a comparison could also be made between the flow down either side of the wind tunnel.

The same general areas were examined when the cloud maker was used. It proved advantageous to also examine the flow along and around the front wall and outside discharge doors.

V. ANALYSIS OF THE INSTRUMENTATION UNCERTAINTIES AND THE PROPAGATION OF THESE UNCERTAINTIES IN THE VELOCITY CALCULATIONS

The main purpose of this investigation was to map the velocity at successive cross-sectional planes in the test section of the wind tunnel. To calculate the desired result, the pertinent parameters must be first identified and then measured. Therefore, the functional relationship between variables must be known. The functional relationship for velocity is:

$$V = \sqrt{\frac{2g\, h_{man}\, \rho_{man}}{\rho_{air}}} = \sqrt{\frac{2g\, R\, T_{air}\, \rho_{man}\, h_{man}}{P_{st}}}$$

where $\rho_{air} = \dfrac{P_{st}}{R\, T_{air}}$

V = velocity (ft/sec)

g = gravitational constant (32.3 ft/sec^2)

h_{man} = height of manometer fluid measured as a result of dynamic pressure (ft)

ρ_{man} = density of manometer fluid (Lb_m/ft^3)

ρ_{air} = density of air in jet (Lb_m/ft^3)

P_{st} = static pressure (Lb_f/ft^2)

R = gas constant $\left(53.3 \dfrac{ft\text{-}Lb_f}{Lb_m\text{-}^\circ R}\right)$

T_{air} = temperature of air in jet ($^\circ R$)

It was postulated at the start, that the velocity would be calculated with an uncertainty level of less than 1% of the calculated velocity with (20:1) odds or a confidence level of 95%. To be able to assign an uncertainty level to velocity, it must first be determined what uncertainty there is in the measurement of each variable. Therefore, in effect, what the experimenter does is to match the instrumentation to a particular experiment to achieve a desired result.

The parameters measured were dynamic pressure, an air stream temperature, and the static pressure. The instruments used to measure each variable respectively were: Micromanometer, glass thermometer and a mercury barometer. From an investigation of instrumentation,[3,4,5] manufacturers' literature, and consultation with other experimenters an uncertainty was arrived at for each instrument. They were as follows:

Micromanometer - $\pm$ 0.0001 in. But. Al. (20:1)

Thermometer - $\pm$ 1.3°R (20:1)

Mercury Barometer - $\pm$ 3.54 Lb/ft^2 (20:1)

These uncertainty levels were determined in the following manner: The micromanometer's uncertainty was obtained from manufacturers' literatures; the thermometer's uncertainty was obtained by taking one half the smallest scale division and adding to it an amount equal to the difference between stagnation and static temperature. The smallest scale division was two degrees, therefore one half of that amount would be one degree. The stagnation minus static temperature must be calculated at the air stream velocity. Since testing was initiated at 66,000 CFM or approximately 60 ft. per second, this value of velocity was used in the calculation. It may further be noted that this uncertainty

specified for temperature measurement in the air stream is the worst possible condition that could occur using the prescribed thermometer in a steady-state flow. The stagnation minus the static temperature is calculated as follows:

$$T_o - T = \frac{V^2}{2KC_p}$$

at 60 ft/sec

$$T_o - T = \frac{(60)^2}{2(1556)(32.2)(.24)} = .3^\circ R$$

where T_o = stagnation temperature ($^\circ R$)

T = static temperature ($^\circ R$)

V = air stream velocity (ft/sec)

C_p = specific heat at constant pressure = $0.24 \frac{BTU}{Lb_m - ^\circ R}$

K = dimensional constant

The total uncertainty for the temperature measurement in the air stream is therefore $1.3^\circ R$. The uncertainty for the barometer was taken to be one half the smallest scale division which in this case was 0.05 in. Hg. or 3.54 Lb/ft^2.

It now becomes necessary to determine how the uncertainty of each measured variable adds to the uncertainty of the calculated velocity. It became evident at the start of testing that the error involved in the process was much greater than the error involved in the micromanometer. At this time it was decided to take ten measurements of pressure at each location and use plus or minus two standard deviations of these ten readings as the uncertainty of the manometer measurements. It might be noted that plus or minus two standard deviations is equivalent to just slightly greater than a 95% confidence level.

From a method first proposed by Kline and McClintock,[2] it can be seen that if V is the velocity:

$$\Delta V = \left\{ \left[\left(\frac{\partial V}{\partial T_{air}} \right) \left(\Delta T_{air} \right) \right]^2 + \left[\left(\frac{\partial V}{\partial h_{man}} \right) \left(\Delta h_{man} \right) \right]^2 + \left[\left(\frac{\partial V}{\partial P_s} \right) \left(\Delta P_s \right) \right]^2 \right\}^{\frac{1}{2}}$$

where

$$V = \sqrt{\frac{2g\, R\, T_{air}\, \rho_{man}\, h_{man}}{P_s}}$$

$$\frac{\partial V}{\partial T_{air}} = \frac{V}{2T_{air}}$$

$$\frac{\partial V}{\partial h_{man}} = \frac{V}{2h_{man}}$$

$$\frac{\partial V}{\partial P_s} = \frac{-V}{2P_s}$$

ΔT_{air} = uncertainty of air stream temperature = $\pm$ 1.3°R

Δh_{man} = uncertainty of manometer measurements = $\pm$ 2 (standard deviations)

ΔP_s = uncertainty of barometer measurements = $\pm$ 3.54 Lb/ft^2

Dividing ΔV by V :

$$\frac{\Delta V}{V} = \left[\left(\frac{\Delta T_{air}}{2T_{air}} \right)^2 + \left(\frac{\Delta h_{man}}{2h_{man}} \right)^2 + \left(\frac{\Delta P_s}{2P_s} \right)^2 \right]^{\frac{1}{2}} \qquad (1)$$

The uncertainty in the velocity ΔV, is therefore equal to $\Delta V/V$ from eq. 1 times V, in ft/sec. It may be noted that the confidence level used for each measurement must be the same when this method is used, also that it yields the same confidence level for the result.

If typical values for the micromanometer reading, air stream temperature and barometric pressure are substituted in Eq. 1 along with an appropriate uncertainty level for each measured parameter, the uncertainty in velocity, expressed as a percentage, is obtained. The quantities inside the radical of Eq. 1 must be in absolute units. Therefore, when the magnitude of each quantity is investigated as to its contribution to the total, the required accuracy for the measurement of each parameter can be determined.

Eq. 1 provides for the choice of instruments to produce a desired result and a means to calculate the uncertainty of that result.

For a standardized day of 70°F and 14.7 psi, the equation for velocity becomes:

$$V = \left(\sqrt{\frac{2g\,R\,T_{sd}}{P_{sd}}}\right)\left(\sqrt{\frac{h_{man}\,T_{air}}{T_{sd}}\,\frac{P_{st}\,\rho_{man}}{P_{sd}}}\right)$$

where

T_{sd} = 70°F or 530°F

P_{sd} = 14.7 psi or 2120 Lb/ft^2

VI. DISCUSSION AND RESULTS

A. Presentation of Calculated Velocities With Accompanying Uncertainties

The velocities presented in Table I were calculated for a flow rate of approximately 66,000 CFM. The location and uncertainty associated with each point in the test section are presented with a 95% confidence level. The first series of velocities presented in the table were taken at the exit plane along the horizontal and vertical center lines. It can be seen from the values obtained for the horizontal traverse that the velocity increases slightly in a symmetrical manner about either side of the center point (1-A). The maximum range in readings along the horizontal is 0.7085 ft. per second. The maximum range for the vertical readings is 1.1934 ft. per second. In general, it can also be seen that the readings along the vertical center line are not symmetrical in nature as are the horizontal velocities. It appears as though the velocities are approximately .7 - .8 ft. per second larger on the lower half of the vertical center line; that is, from the mid point down on Fig. 5.

After the exit plane had been mapped as far as pressure readings were concerned, it was noticed that the outer boundary of the fan appeared to be above the wind tunnel center line. Measurements were taken, and the wind tunnel raised 2 3/4 in. so that its center line corresponded to the center line of the fan. Flow parameter measurements were again taken at the exit plane and the corresponding velocities presented as the second series of values in Table I. The same symmetry in flow characteristics can be seen with respect to the

horizontal center line. The maximum range of values are 0.9136 ft. per second along the horizontal center line and 1.5977 ft. per second along the vertical center line. The range of values appears to be much greater than the symmetry of values would first indicate. This is due to the value at point (1-C') on the vertical traverse, which is considerably lower than the rest of the calculated velocities.

It appears that raising the wind tunnel 2 3/4 in. had the effects of: producing a more symmetrically distributed flow; and increasing the values of velocity slightly for corresponding locations due to less pressure loss in the diffuser section of the wind tunnel.

It was decided to leave the wind tunnel at the elevated location for all further measurements. The same flow parameter measurements were taken at 1 1/2 ft. away from the exit plane and the calculated velocities are presented as series three in Table I. Again the tendency for the velocity to increase outwardly along the horizontal center line can be seen. The maximum range on the horizontal center line is 0.4748 ft. per second. The velocities along the vertical center line are symmetrically distributed about the center point (1-A), with the tendency to increase in either direction out from the center line. The maximum range of values on the vertical center line was 0.7978 ft. per second.

In a comparison of the exit plane and 1 1/2 ft. away from the exit plane, it can be seen that the range of values along the vertical and horizontal center lines, and the symmetrical distribution of flow is better at the 1 1/2 ft. location. It was felt that the constant pressure boundary around the jet caused this increased uniformity

of flow.

It was the intention of this investigation to map successive cross sections at both high and low flow rates. Unfortunately, when measurements were attempted at a location 3 ft. away from the exit plane, the micromanometer could not respond to the fluctuations that were encountered in the flow. It then was decided to abandon further pressure measurements in favor of an investigation into the cause of these fluctuations. The results of this investigation will appear in several of the following sections.

B. Photographic Study with the Grid-and-Tuft Scheme

A photographic study using a grid-and-tuft scheme was undertaken to visually examine the flow at succeeding cross sections in the test section. It was felt that this investigation could be correlated with the pressure measurements for the same flow rates and locations.

Two flow rates were examined in an attempt to compare the flow patterns. The high inlet damper setting used was exactly the same setting used for the pressure measurements, and hence calculated velocities. A 3/4 closed inlet damper setting was chosen for the lower flow rate.

It should be noted that the photographs were taken with the wind tunnel in the 2 3/4 in. raised position and that the 4 ft. by 4 ft. exit area of the wind tunnel corresponds to 12 spaces or 13 grid wires in the photographs (i.e., the grids are 4 in. on a side). The center of the test section can be located by drawing diagonal lines across opposite corners of the exit area of the wind tunnel, shown in the background of each photograph. After the center is located, the

steady flow region can be obtained by counting the appropriate number of 4 in. grid spaces in either direction. It might be added that motion or turbulence in these photographs will show up as a blur at the end of the yarn tufts.

Fig. 6 shows the flow to be quite steady at the exit plane for the high inlet damper setting. Very little motion can be distinguished inside the 4 square ft. exit area of the tunnel. The motion that is seen at edges of the exit area is due to the beginning of turbulent mixing between the jet and the still air in the room. Fig. 7 shows the flow at the exit plane for the low damper setting. There is no apparent distinguishable difference between the flow in Fig. 6 and Fig. 7 with all the same characteristics present.

Fig. 8 shows the flow pattern at 1½ ft. away from the exit plane for the high inlet damper setting. The flow also appears to be quite constant at this location. But it is observed that the turbulent mixing as started to move in toward the center, and motion is detectable on the grid 4 in. in from the 4 ft. square on all sides. However, there is a core 40 in. square of stable flow remaining. Fig. 9 shows the same location for the low inlet damper setting. Again, both photographs show exactly the same flow characteristics.

In making a comparison between the flow visualization and pressure measurements or calculated velocities at the exit plane and the 1½ ft. location, the relatively small values of standard deviation obtained for the dynamic pressure (see Appendix D) over approximately a 40 square in. area indicates that the time variance of the pressure readings was small. This correlates with the photographs taken at

these locations and indicates a steady flow.

Fig. 10 shows the flow pattern 3 ft. from the exit plane for the high inlet damper setting. It can be seen from this figure that a stable core of only approximately 24 square in. remains. The turbulence level at this location appears to have increased drastically over what it was for the 1½ ft. location. It is felt that the turbulence at this cross section could have some bearing on the fluctuations encountered during pressure measurements.

Fig. 11 shows the flow pattern at the 3 ft. location for the low inlet damper setting. It can be seen from this figure that more turbulence exists for this damper setting than did for the higher setting. This result is expected and will occur in any open-jet.

As the flow rate is reduced, mixing penetrates the flow to a greater extent and usually occurs closer to the exit plane of the wind tunnel. The stable core in Fig. 11 appears to be reduced to 16 square in.

Fig. 12 shows the flow pattern 4 ft. from the exit plane for the high inlet damper setting and indicates about the same conditions as for the 3 ft. station at the same damper setting. A 12 in. square core remains, however, some violent turbulent motions can be observed at the 4 square ft. boundary area.

Fig. 13 shows the flow pattern 4 ft. from the exit plane for the low inlet damper setting. More turbulence is visible near the center of the flow and for all practical purposes the core is reduced to about an 8 in. square.

From the grid-and-tuft study, it can be seen that for the most

part the same flow stability is discernible at both the high and low inlet damper settings.

C. Circulation Study

A circulation study was performed in the wind tunnel room. Fig. 2 shows the relative position of the wind tunnel in the laboratory. It was felt that the combination of this off-centered location and the double entry from the adjoining room and hallway may cause an unbalanced circulation of air in the room.

The wind tunnel draws most of its intake air from the room, and while running strong air currents are noticeable around the inlet to the fan. A qualitative understanding of these air currents was deemed important.

The grid-and-tuft network was moved around the room and photographed to record these air currents. Fig. 16 shows the grid-and-tuft network set in the double doorway of the adjoining room. No measure of the quantity of flow is available, but it can be seen that the predominant direction of flow is toward the inlet of the fan. The right end of the frame for the grid was then rotated 90° clockwise and moved along the left side of the tunnel a few feet. The upper photograph in Fig. 17 shows this location. In comparison, the flow is seen to be almost negligible. A significant number of yarn tufts are left hanging in a vertical manner signifying little or no flow. The grid system was then moved to the right side of the tunnel and placed at approximately the same position from the rear wall as when it was on the left side. The lower photograph in Fig. 17 shows the flow pattern at this location. It can be seen from the tuft locations that a

sizeable amount of air recirculates along the right side of the wind tunnel.

A cloud maker was used at the same locations in the room with the same results. However, the cloud maker allowed the flow to be visualized near the exit window in the front wall. It was observed that the bulk of the jet exited out through the opening but with some flow traveling in a horizontal direction along the front wall above and below this exit.

In summary, it can be said that most of the circulation currents occur from the adjoining room and along the right side of the wind tunnel with the one from the adjoining room being the stronger.

D. Air Stream Fluctuation Study

As previously mentioned, a fluctuation in the air stream was encountered at a cross-sectional plane 3 ft. from the exit plane during pressure measurements. A study of the frequency and amplitude of this fluctuation on the axial center line of the test section and along the horizontal center line at the 3 ft. cross section was conducted. The micromanometer and pitot-reference frame combination were used for this study. A three-minute period was chosen to count these fluctuations as it was observed they did not occur in a periodic fashion. That is, several fluctuations were observed followed by a period of no motion. A stop watch was used to keep time over three three-minute time intervals yielding an average period. The amplitude was obtained by placing marks on the inclined glass tube of the micromanometer at the end points of these fluctuations. The natural frequency of the micromanometer was calculated to be approximately 1.14 cycles per

second. This was done so as to distinguish between the frequency observed in the air stream and that occurring in the manometer.

Fig. 14 shows the plotted results of this study as measured along the axial center line of the test section. It is observed that an increase in the slope of this curve between the 1 1/2 ft. and 3 ft. distances. A peak occurs at approximately 3 1/4 ft. from the exit plane. It may be further noted that all points observed had approximately the same amplitude of 0.0150 in. of butyl alcohol. This amounts to about 3/4% on velocity. The reason this percentage difference did not appear in the readings at the 1 1/2 ft. location can be seen by the number of cycles that occurred in one minute at that location. It becomes apparent that the micromanometer readings were taken when the flow appeared stable between fluctuations.

Fig. 15 shows the results of the horizontal traverse along the center line. This study was performed one week later than the one shown on Fig. 14. The important thing to note here is that although there is a wide variety of frequencies present across the width of the jet; the center line point measured to be exactly what it was on Fig. 14. The center point measurement was obtained first, then points in succession moving toward the right. The center point was measured again and then points to the left were taken in succession. The center point was then checked again and found to be the same. By ascertaining this center point to be the same on different days under different ambient conditions, it can be concluded that ambient temperature and pressure changes have little or no effect on the period or amplitude of the observed fluctuations.

E. Miscellaneous Studies

The RPM of the fan motor was observed over a 15 minute period to find out whether changes in RPM had any relation to the observed fluctuations. The RPM was found to be constant for this period of time.

The Helmholtz Resonator frequency of the wind tunnel and room was also determined.

The natural frequency of a Helmholtz Resonator is defined to be:

$$\omega_o = \sqrt{\frac{1}{MC}} \quad \text{where}$$

$$M = \text{acoustic inertance} = \frac{\rho_o l'}{S}$$

$$C = \text{acoustic compliance} = \frac{V}{\rho_o C^2}$$

ρ_o = density of the air

l' = effective length

S = cross-sectional area at outlet

V = volume of air inside the wind tunel (or room)

C = speed of sound in air.

The Helmholtz Resonator natural frequency of the wind tunnel was calculated to be 11 cps. This value is well above the 0.0666 cps that was observed in the jet. The room configuration was then used to calculate the Helmholtz natural frequency. The value obtained was 3.38 cps. Different amounts of added volume from the adjoining room and effective lengths were tried with the lowest result being 1.485 cps. This value still being significantly higher than the observed value in the jet.

VII. CONCLUSIONS AND RECOMMENDATIONS

In conclusion, it may be said that the flow is quite stable at the exit plane and at 1 1/2 ft. from the exit plane as was evidenced in the photographic study and by the standard deviations of the pressure measurement readings.

The circulation currents that exist in the room during operating conditions are felt to have some effect on the observed fluctuations in the jet. The fan is placed under an unsymmetrical loading condition by drawing most of its intake air from the adjoining room.

The fluctuation that was measured in the air stream is of the order of 3/4% of the measured velocity. This fluctuation does not become prominent until a location of approximately 2 1/2 ft. from the exit plane. Therefore, if it is at all possible, it is recommended that all testing with models be done at a location of between 1 1/4 ft. and 2 1/2 ft. from the exit plane.

The photographic study showed that it is quite reasonable to expect the same flow characteristics at both a high and low flow rate for locations inside the 3 ft. distance from the exit plane.

An inlet is being designed so that the intake air will be drawn through a duct from an opening in the roof. This new intake system should alleviate most of the adverse circulation currents that now exist in the room. After this new system has been installed, it is my recommendation that this fluctuation study be repeated to determine whether the existing fluctuations still exist. If they do, there are two additional recommendations that can be offered at this time. The

first of these being to construct a plywood room around the test section. This room should be constructed in such a manner that the floor, side walls, and ceiling around the test area are all an equal distance from the center line of the flow. This room should be extended from the exit plane to the opening through the outside wall and should form a smooth transition as it passes through the wall.

The second recommendation would be to do a flow study on the diffuser section of the wind tunnel. It is possible that the flow is not being distributed until it is forced through the perforated plates in the plenum chamber. If this is the case, a truncated cone baffle could be designed to aid the diffuser in distributing flow. It is felt that a more uniformly distributed flow could be achieved by distributing the flow before it reaches the plenum chamber.

VIII. REFERENCES

1. Pope, Harper, Low-Speed Wind Tunnel Testing, Chapter III, Wiley, 1966.

2. Kline, McClintock, "Describing Uncertainties in Single-Sample Experiments", Mechanical Engineering, March, 1953.

3. A.S.M.E. Power Test Codes, PTC 19.2, "Pressure Measurements", Instruments and Apparatus, 1964.

4. A.S.M.E. Power Test Codes, PTC 19.1, "General Considerations", Instruments and Apparatus, 1935.

5. Beckwith, Buck, Mechanical Measurements, Chapter 12, Sections 2, 10, 11, and 17, Addison Wesley, 1961.

6. Flow Corporation, Bulletin No.'s 17A and 19, "Model MM3 Micromanometer - Notes and Instructions", 1963.

7. Kinsler, Frey, Fundamentals of Acoustics, Chapter VIII, Wiley, 1967.

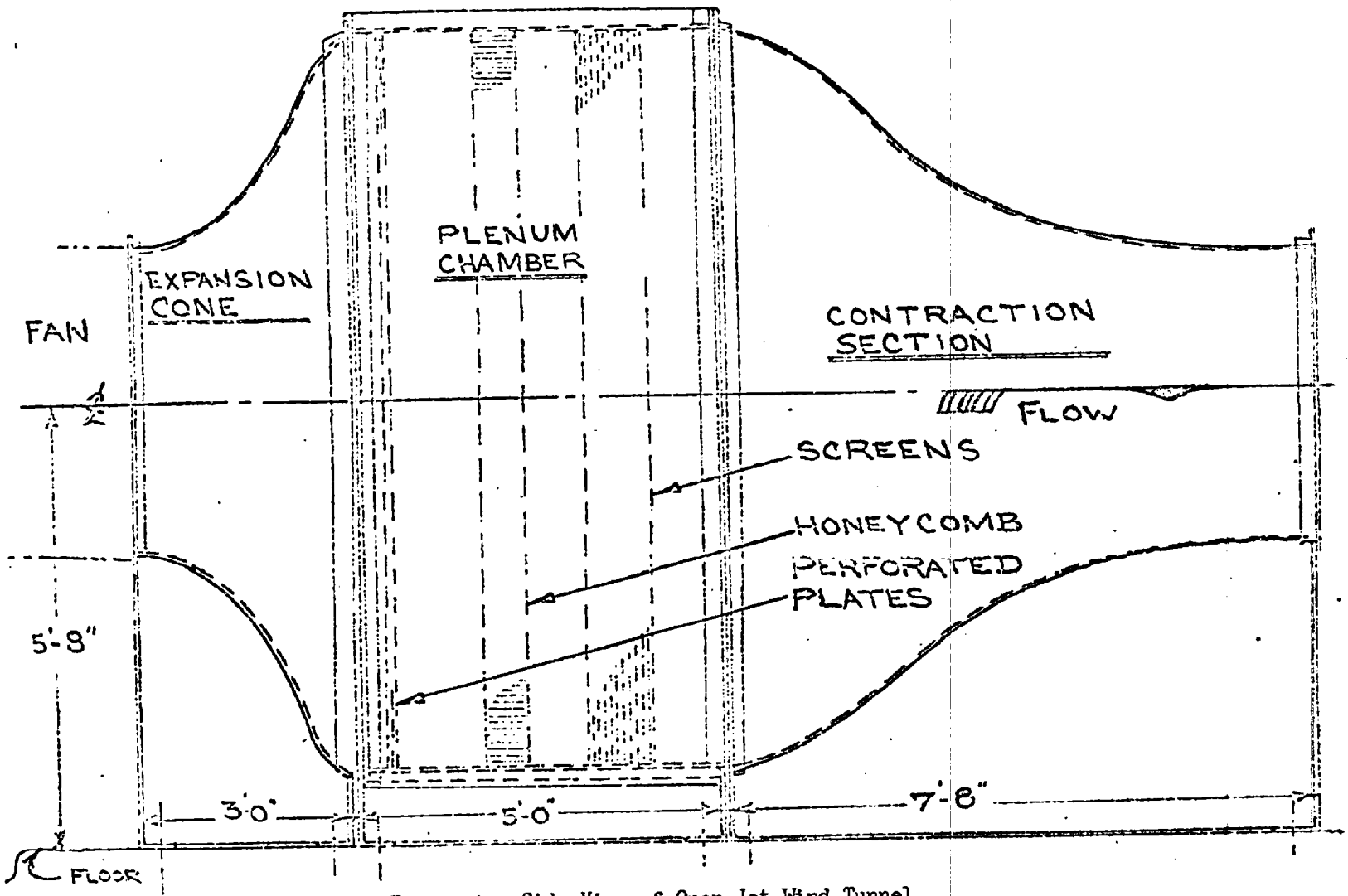

Figure 1 - Side View of Open-Jet Wind Tunnel

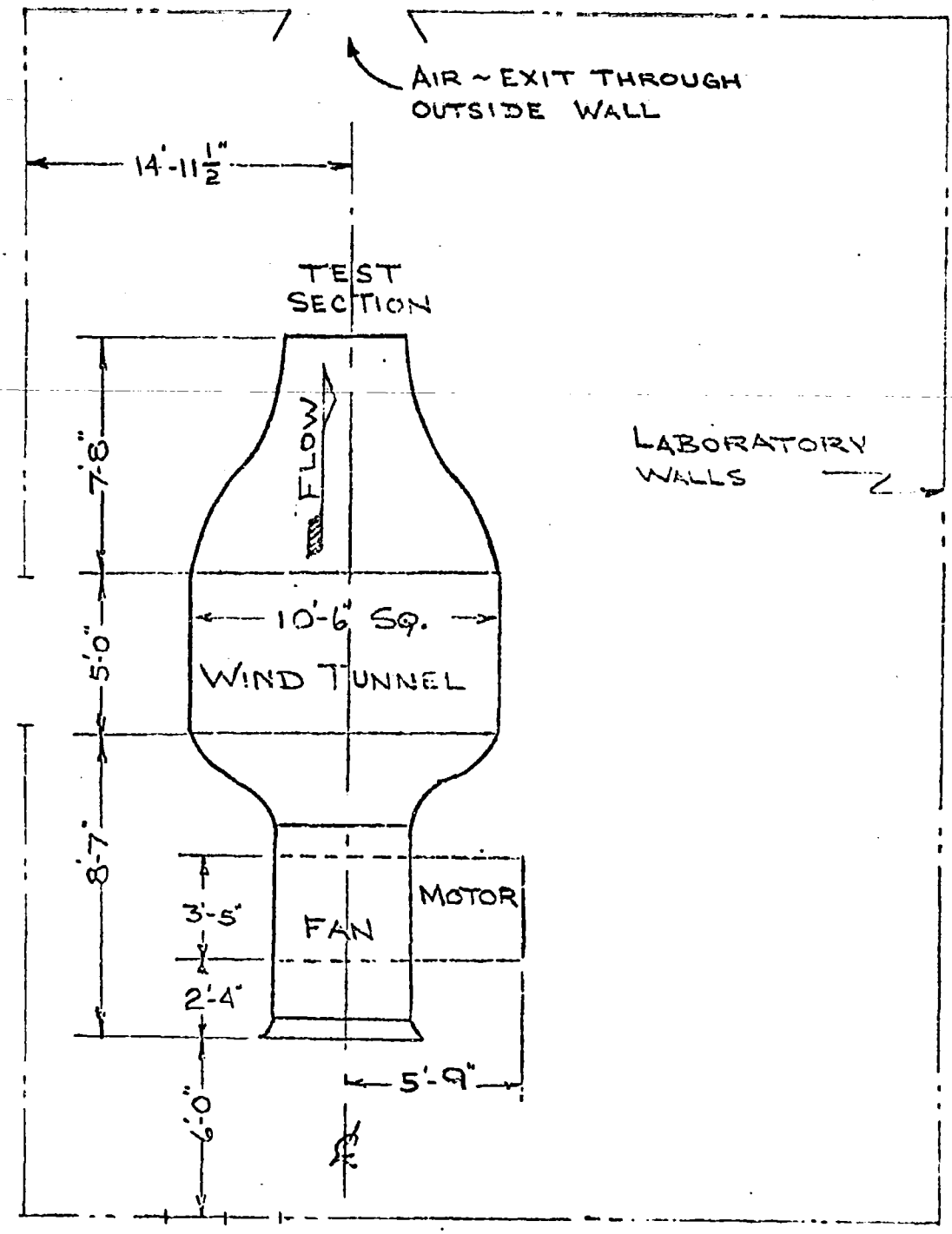

Figure 2 - Fan, Wind Tunnel and Test Section in Plan View

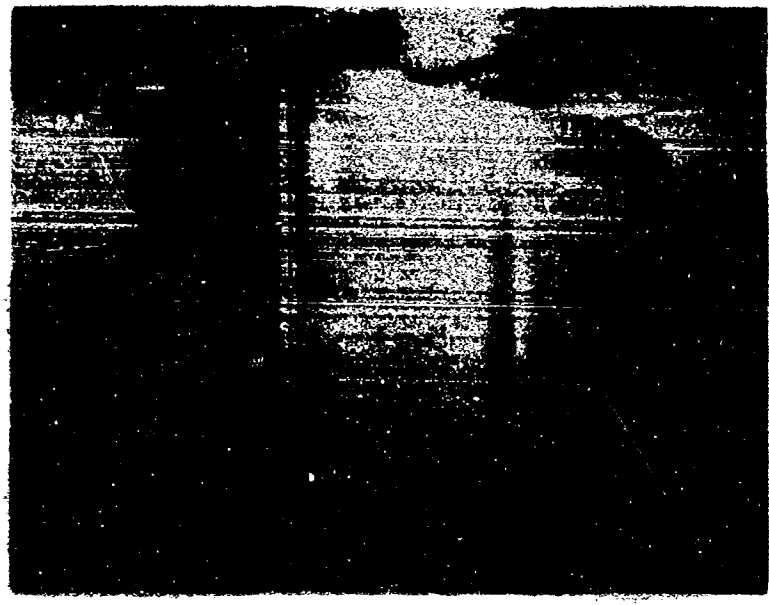

Figure 3. Photograph of Wind Tunnel and Fan

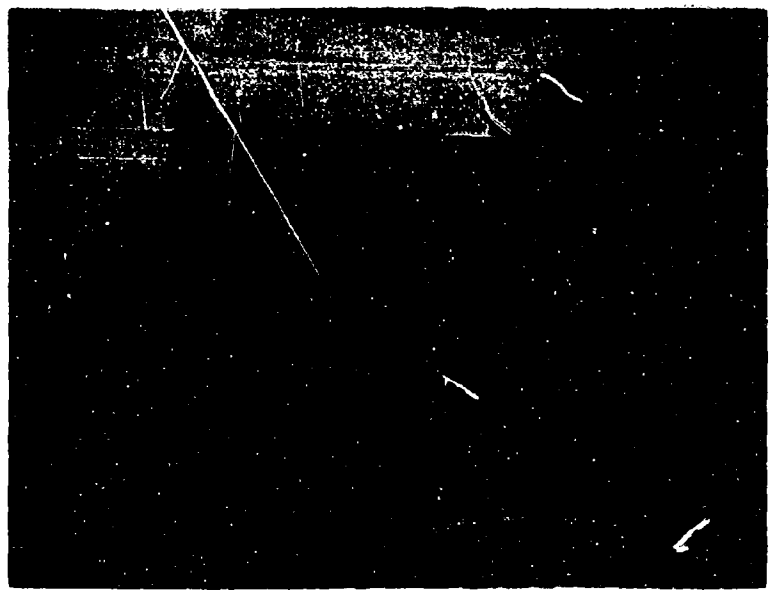

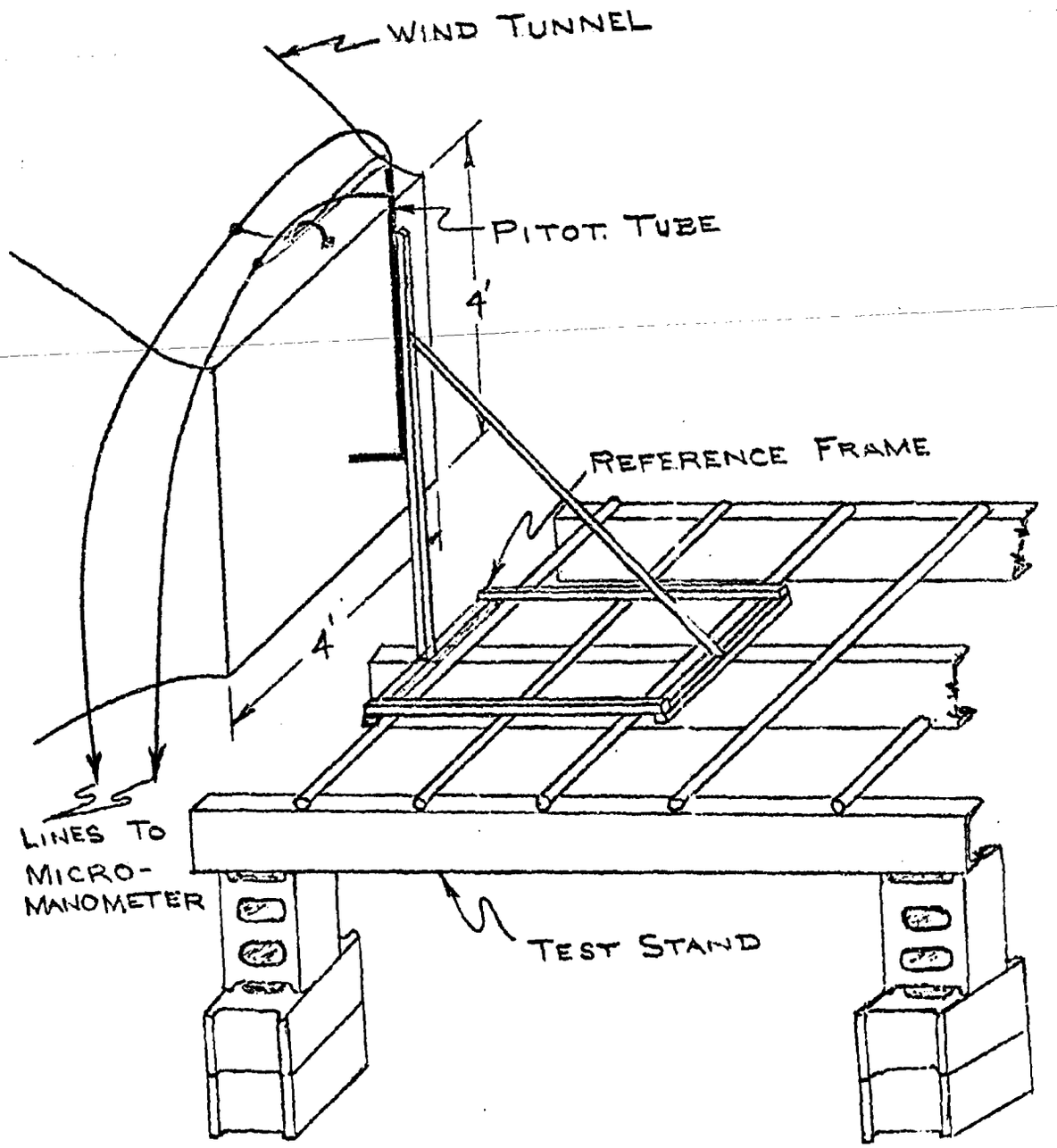

Figure 4 - Schematic Diagram of Air Stream Test Apparatus

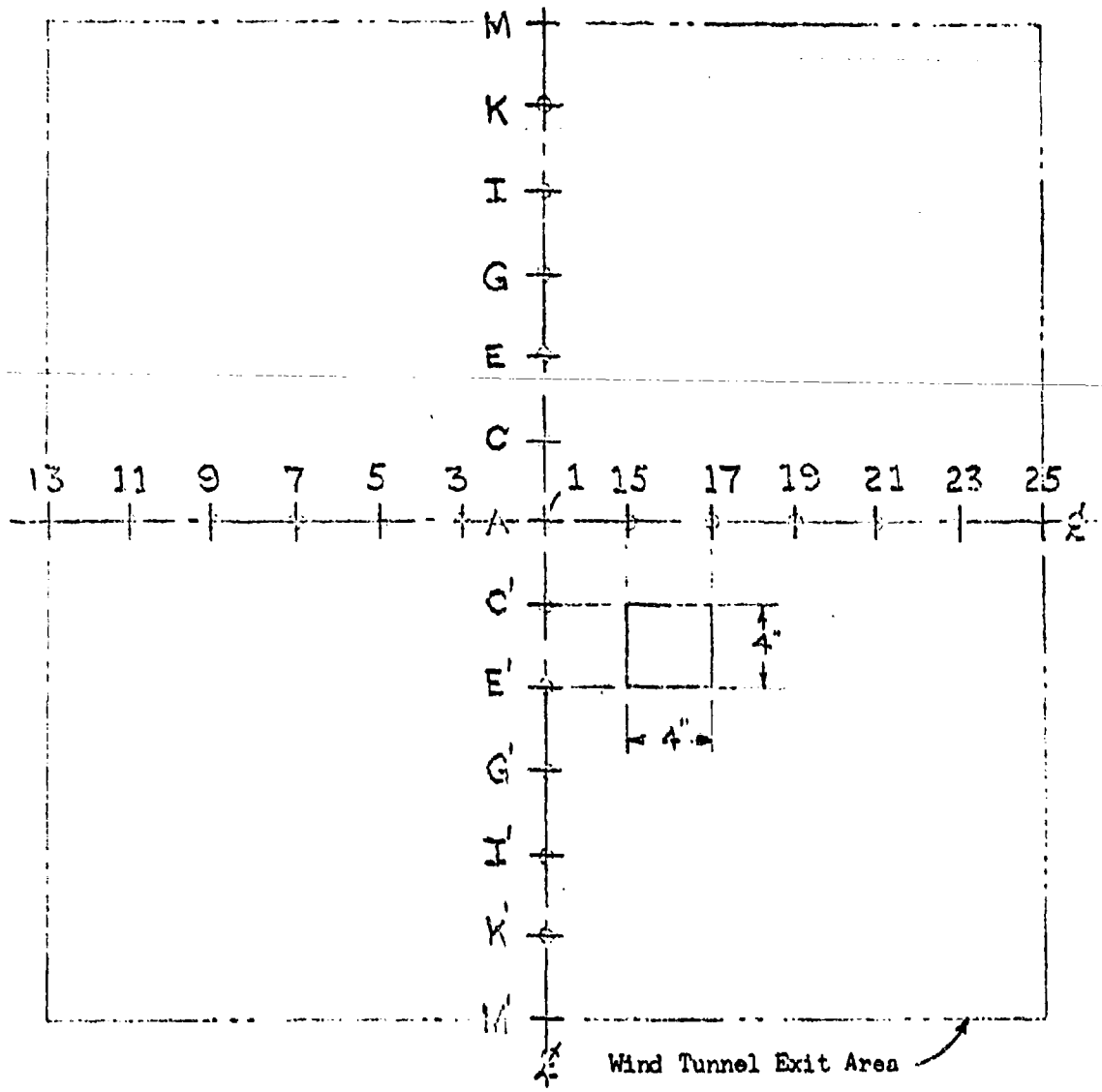

○ Denotes points at which pressure measurements were taken.

Figure 5 - Location of Test Points

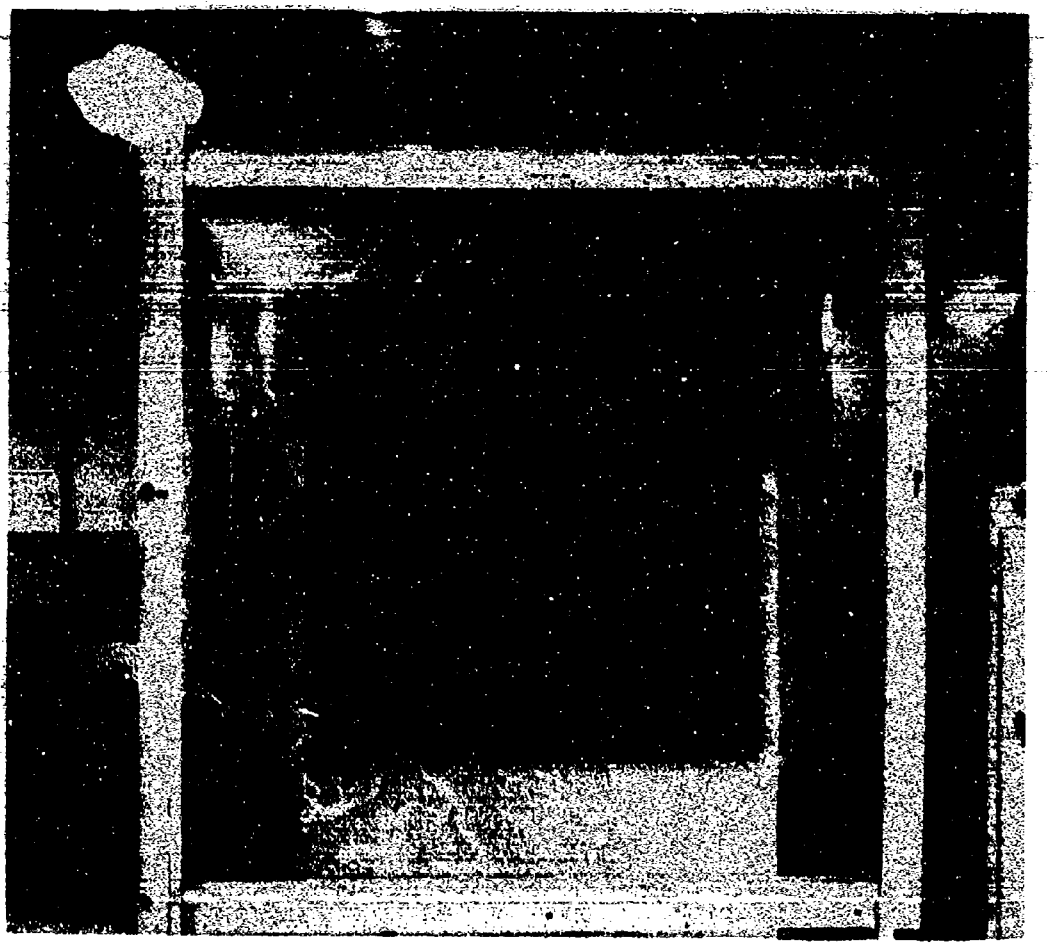

Figure 6. Exit Plane - High Inlet Damper Setting

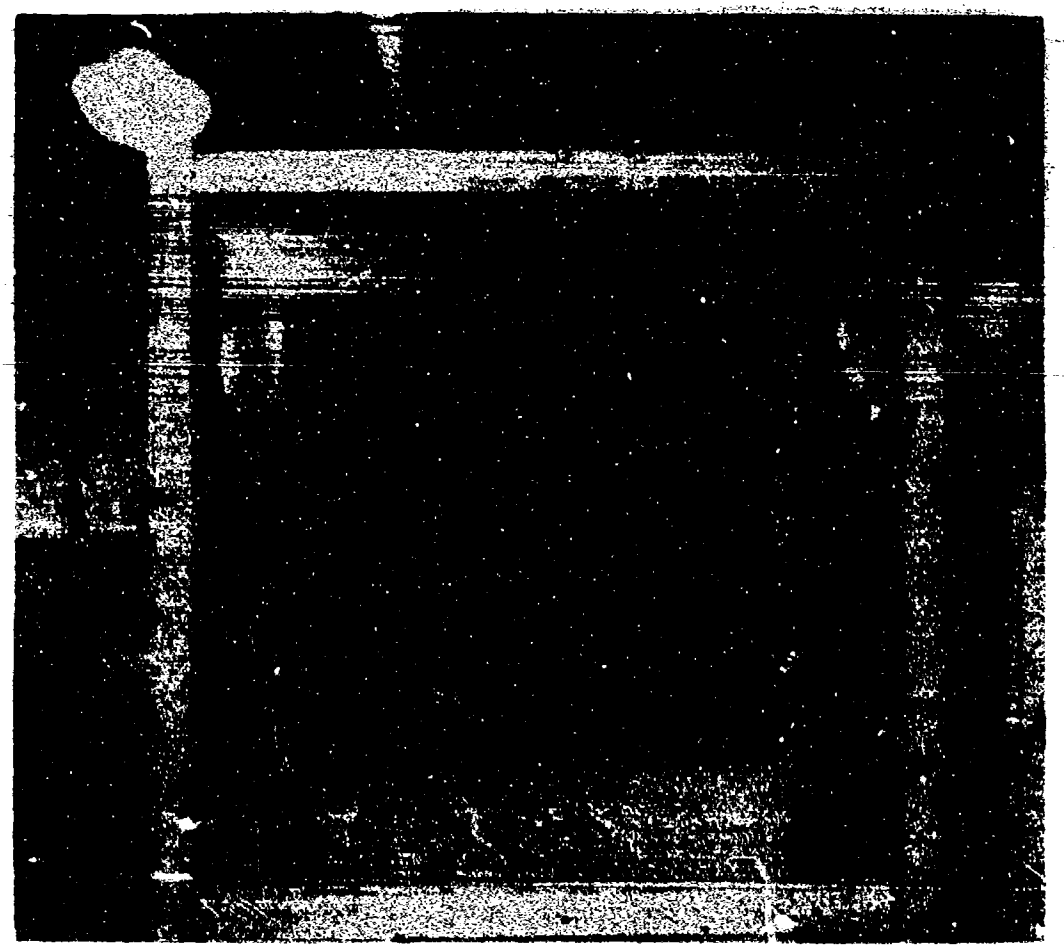

Figure 7. Exit Plane - Low Inlet Damper Setting

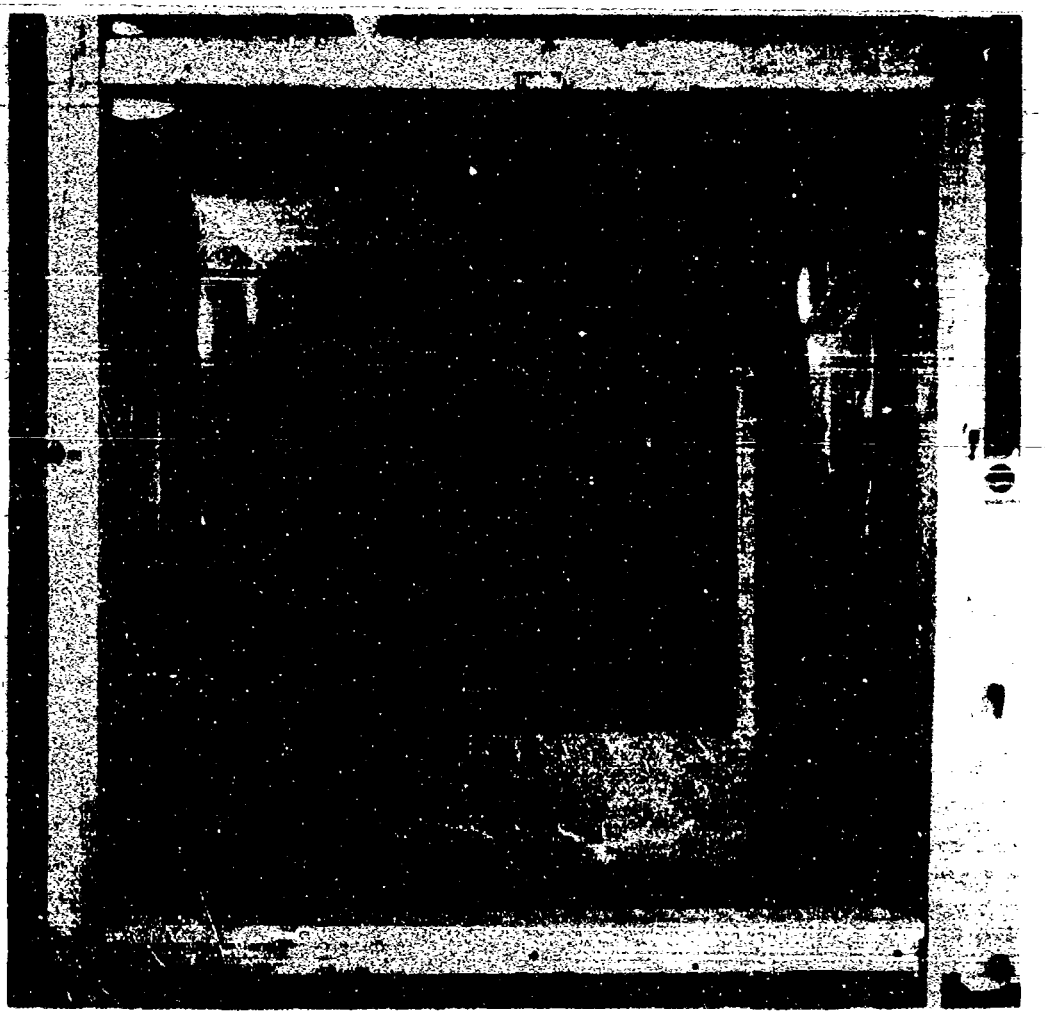

Figure 8. 1½ Ft. Back From Exit Plane - High Inlet Damper Setting

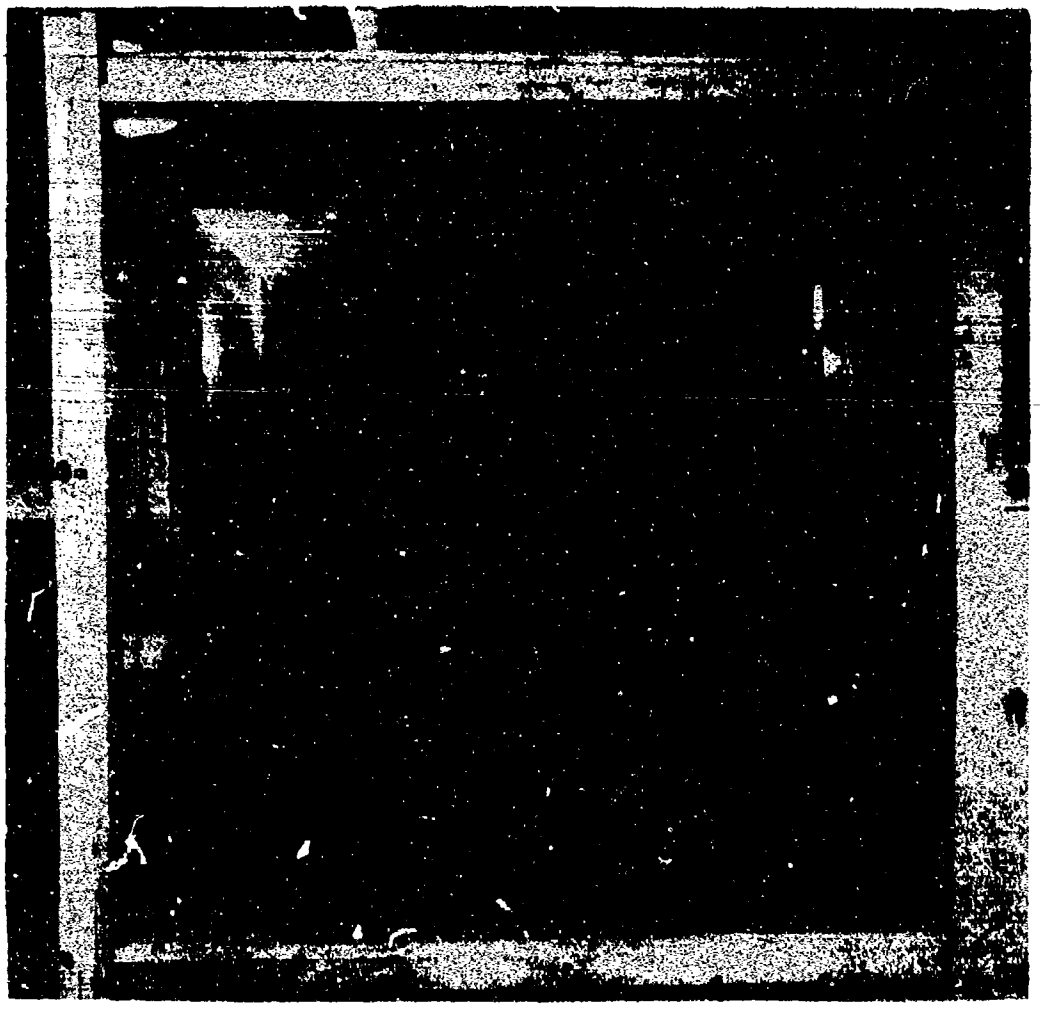

Figure 9. 1½ Ft. Back From Exit Plane - Low Inlet Damper Setting

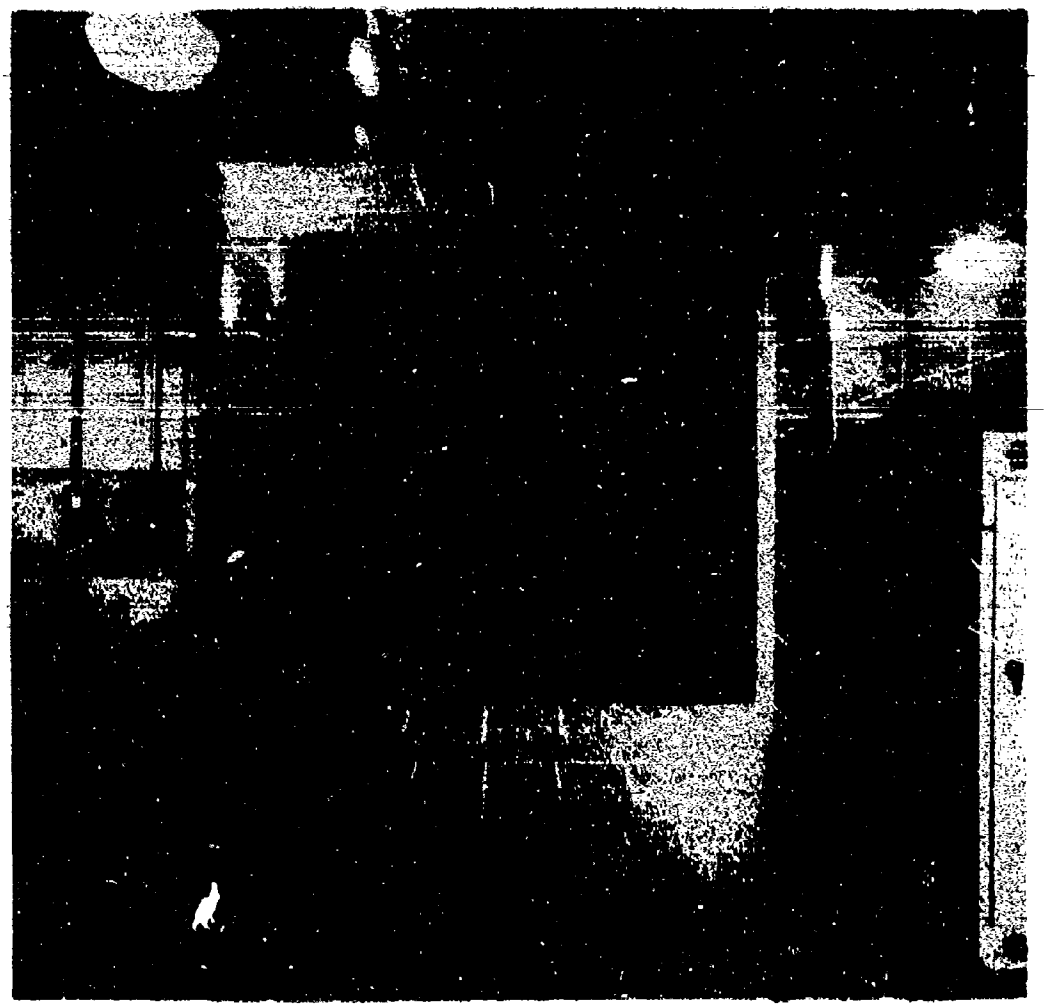

Figure 10. 3 Ft. Back From Exit Plane - High Inlet Damper Setting

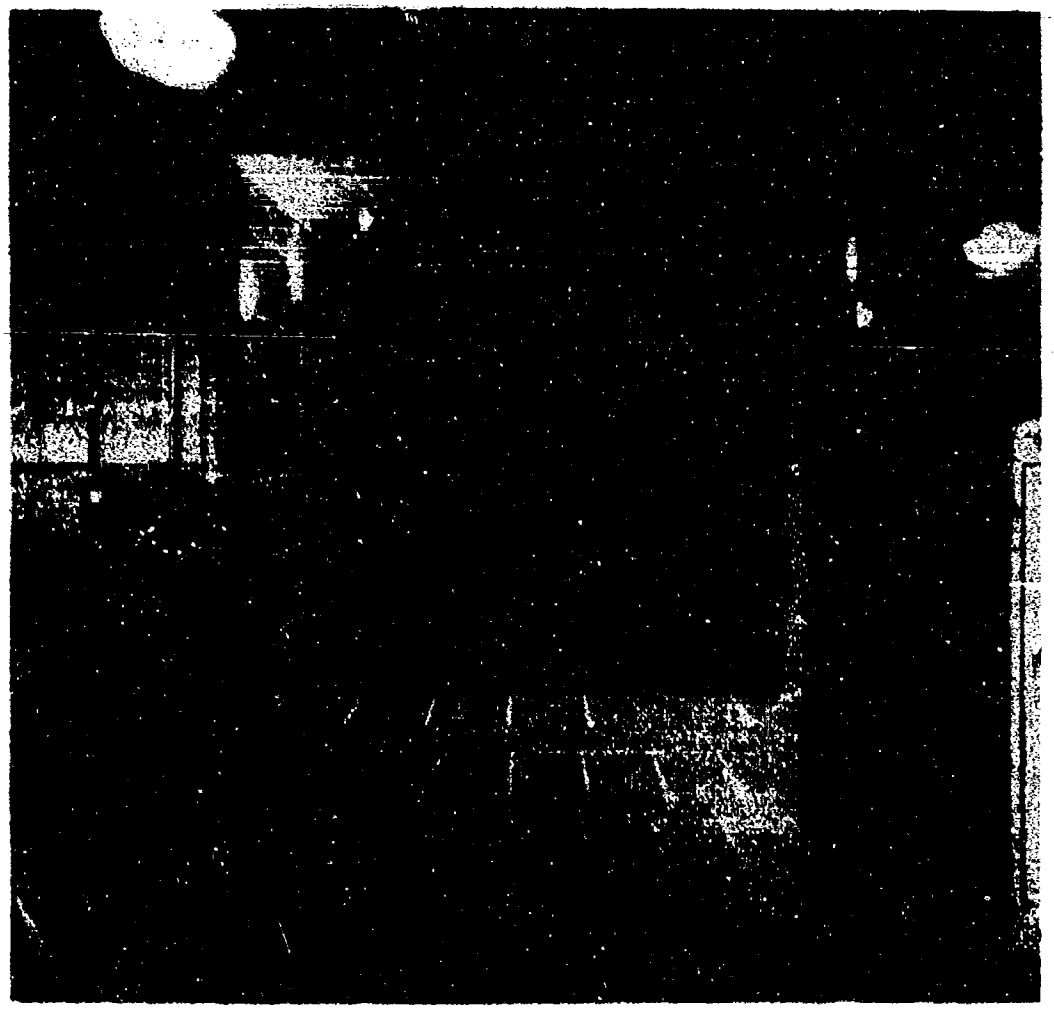

Figure 11. 3 Ft. Back From Exit Plane - Low Inlet Damper Setting

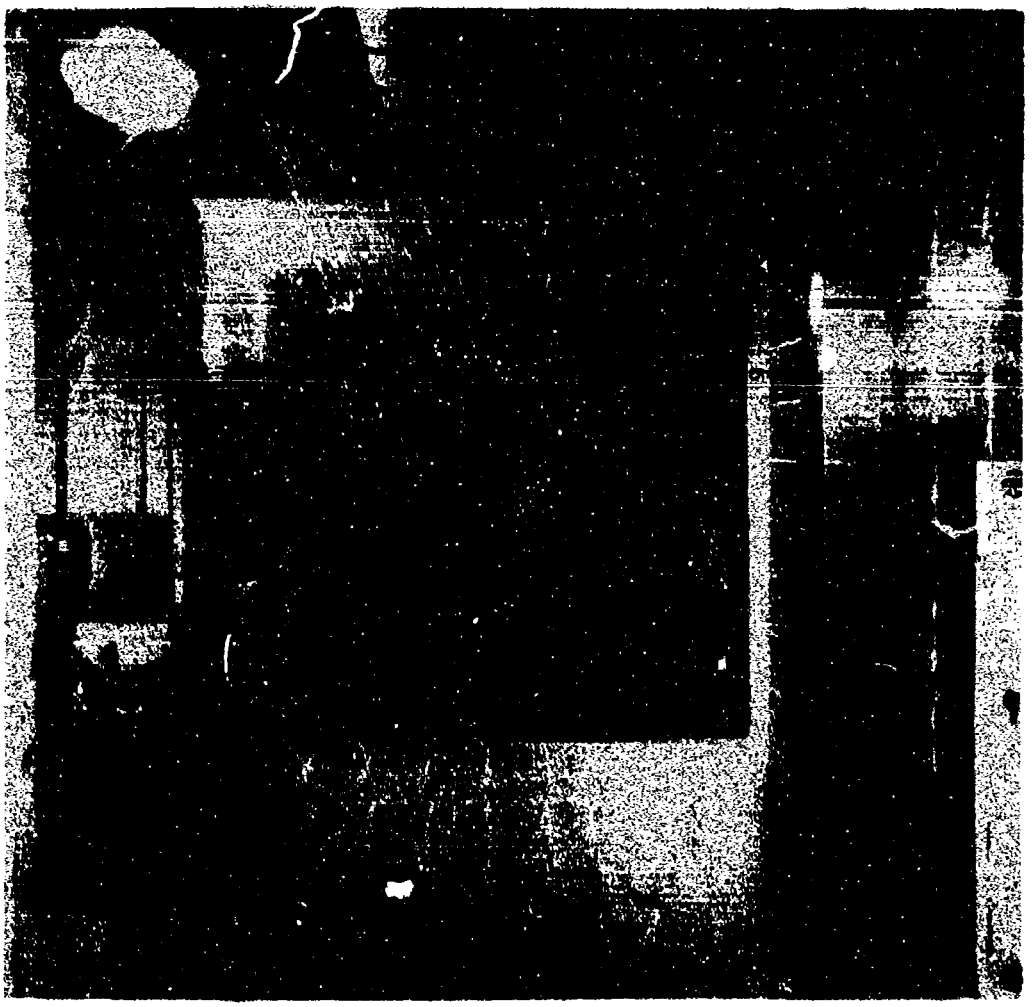

Figure 12. 4 Ft. Back From Exit Plane - High Inlet Damper Setting

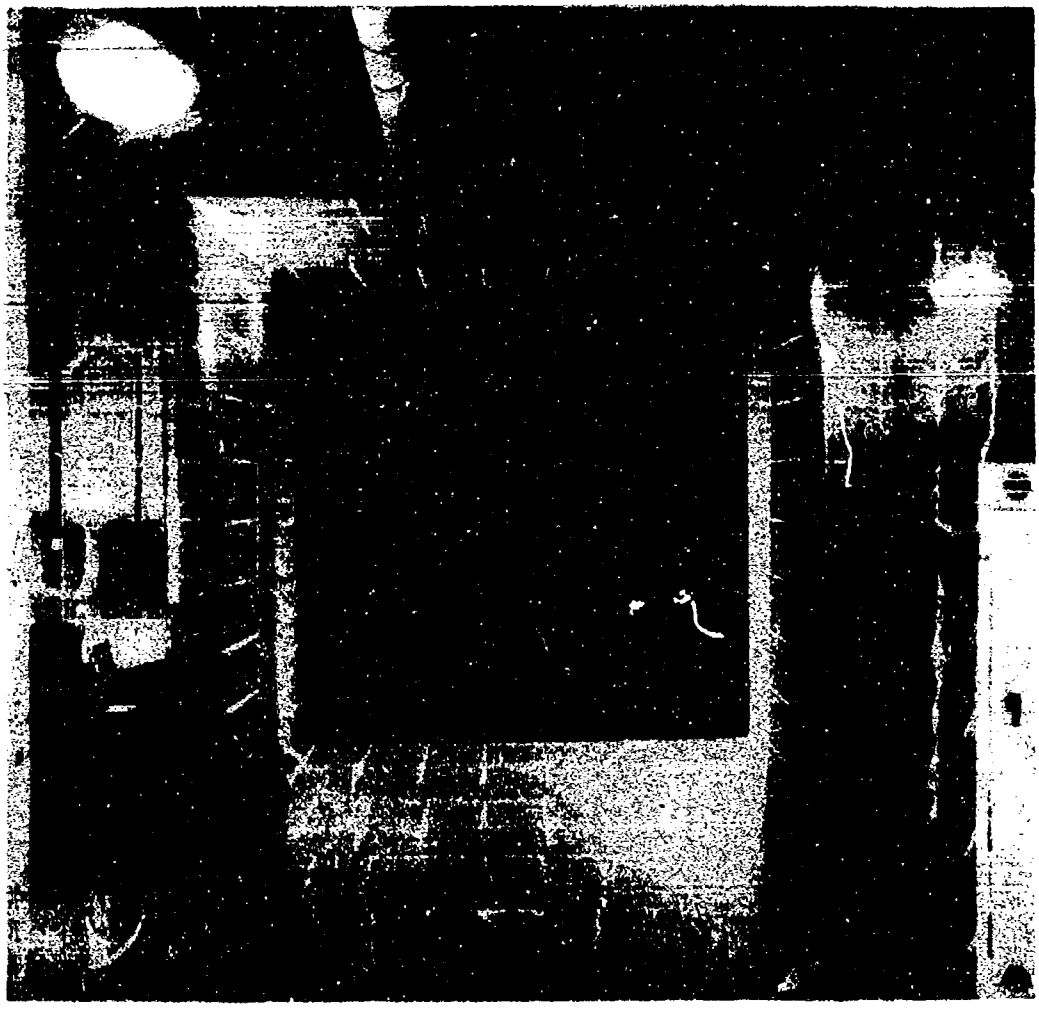

Figure 13. 4 Ft. Back From Exit Plane - Low Inlet Damper Setting

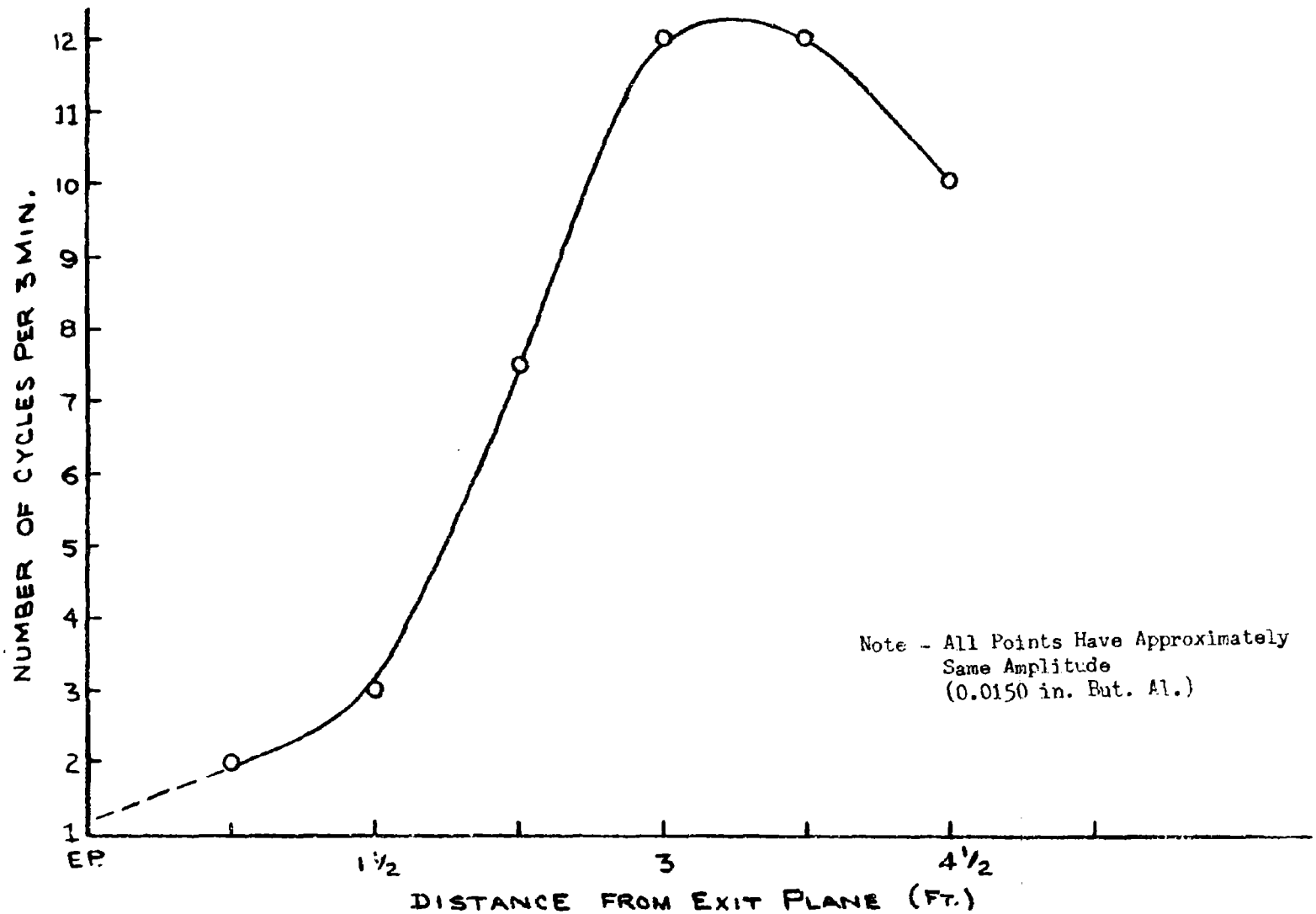

Figure 14. Results of Frequency Study Vs. Distance Out From Exit Plane

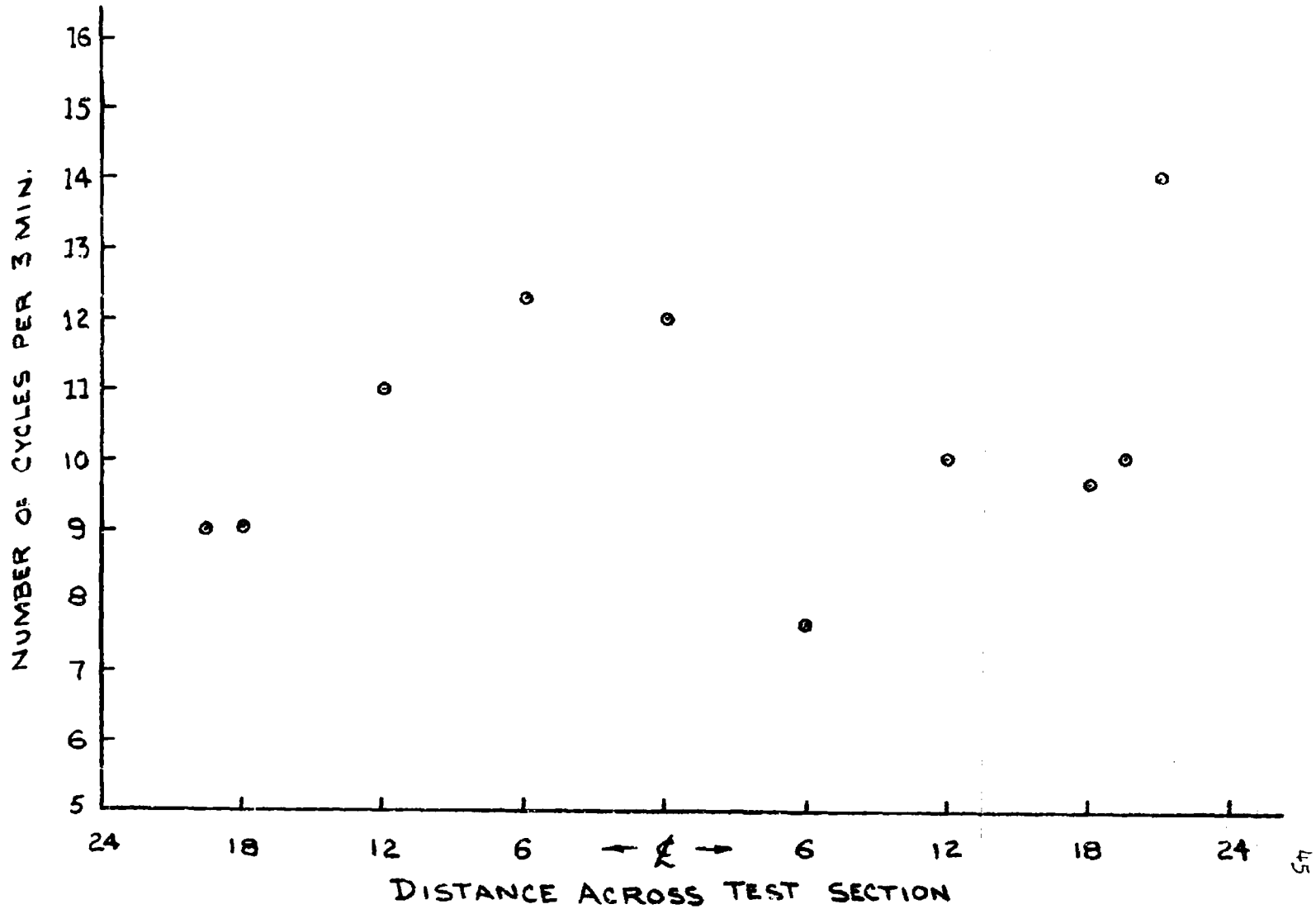

Figure 15. Results of Horizontal Frequency Study at the 3 Ft. Cross Sectional Plane

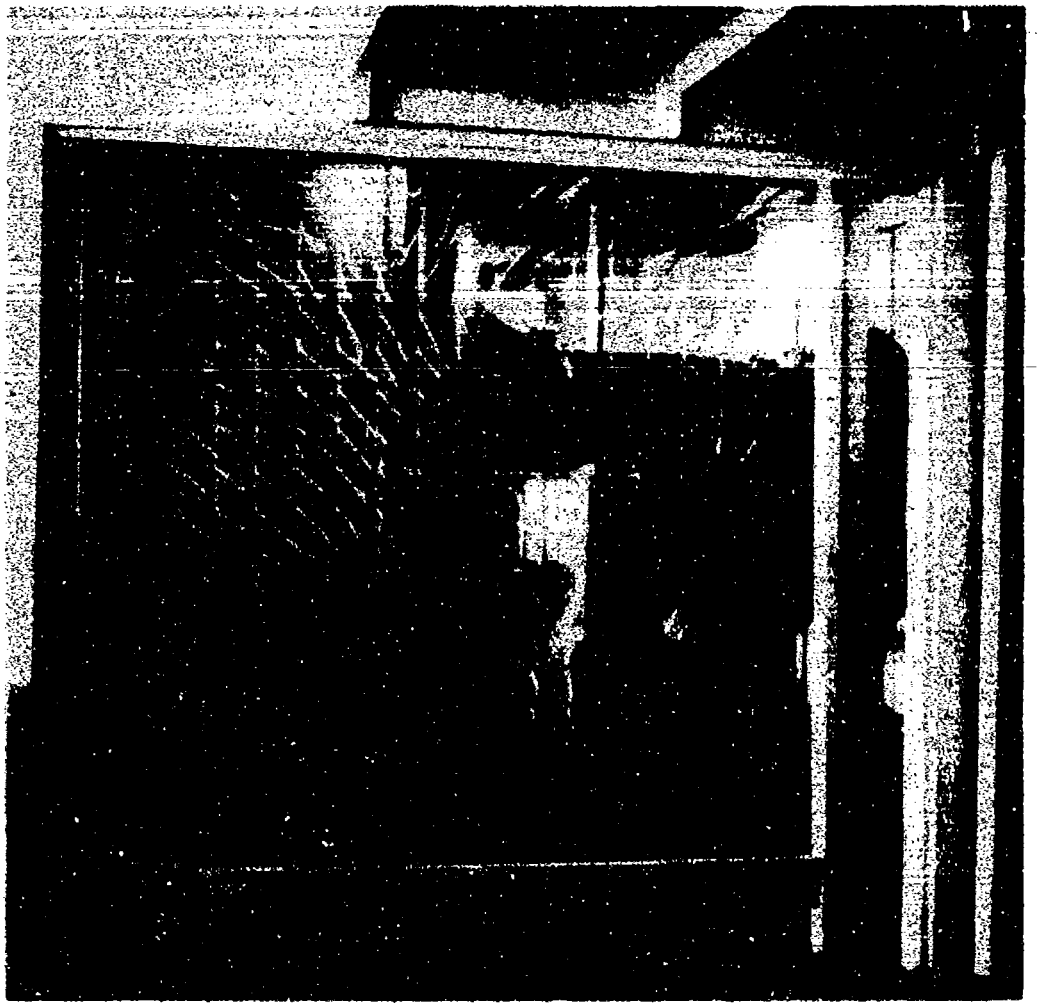

Figure 16. Circulation Study - Flow From Adjoining Room

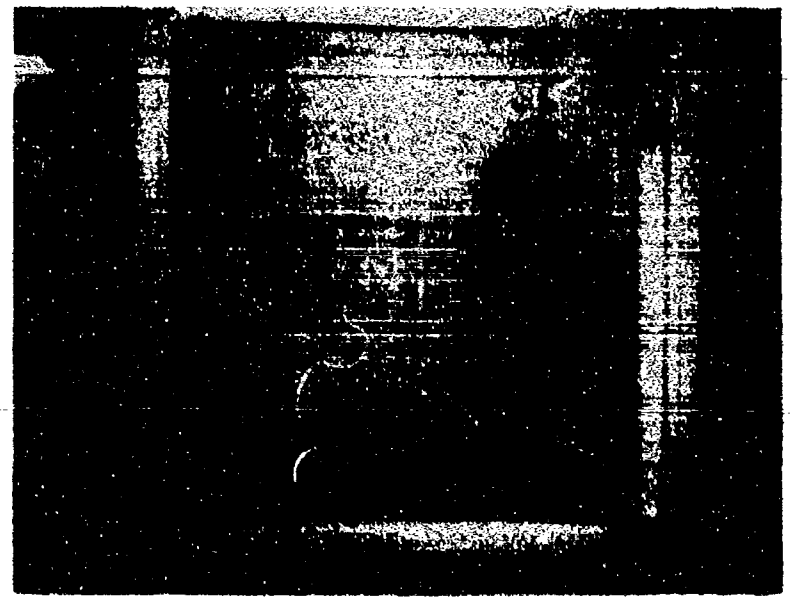

Left Side

Figure 17. Circulation Study - Flow Along Sides of Wind Tunnel

Right Side

TABLE I

Calculated Velocities - Corrected to a Standard Day ($70^{\circ}F$ and 14.7 psia)

Velocities at Exit Plane of Wind Tunnel

For Location of Particular Points - See Fig. 5

(Horizontal Traverse)

Location	Velocity	
1-A	63.8608 ± 0.2952	
3-A	63.9625 ± 0.2334	
5-A	64.2161 ± 0.2337	
7-A	64.4462 ± 0.2406	
9-A	64.6280 ± 0.2280	
11-A	64.5721 ± 0.2781	(20:1)
15-A	63.8721 ± 0.2701	
17-A	64.0331 ± 0.2402	
19-A	64.2470 ± 0.2404	
21-A	64.4406 ± 0.2948	
23-A	64.5693 ± 0.3578	

(Vertical Traverse)

1-C'	63.2980 ± 0.2619	
1-E'	63.1965 ± 0.2086	
1-G'	63.4485 ± 0.4150	
1-I'	63.3171 ± 0.2542	
1-K'	63.7648 ± 0.3291	(20:1)
1-C	62.7946 ± 0.2782	
1-E	62.6674 ± 0.2322	
1-G	62.8525 ± 0.2781	
1-I	63.5168 ± 0.2944	
1-K	63.4157 ± 0.3482	

Velocities at Exit Plane after Raising Wind Tunnel 2 3/4 in.

(Horizontal Traverse)

Location	Velocity	
1-A	64.2455 ± 0.2349	
3-A	64.3143 ± 0.3345	
5-A	64.5372 ± 0.2978	
7-A	64.5087 ± 0.3248	
9-A	64.8674 ± 0.3152	
11-A	65.1591 ± 0.2570	(20:1)
15-A	64.0072 ± 0.2489	
17-A	64.1796 ± 0.3254	
19-A	64.5144 ± 0.2849	
21-A	64.8077 ± 0.2176	
23-A	65.1110 ± 0.4815	

(Vertical Traverse)

1-C'	63.9755 ± 0.4558	
1-E'	64.4401 ± 0.3533	
1-G'	64.5886 ± 0.3434	
1-I'	65.5620 ± 0.2431	
1-K'	65.5732 ± 0.2365	(20:1)
1-C	64.5201 ± 0.3067	
1-E	64.7281 ± 0.3337	
1-G	64.8390 ± 0.5038	
1-I	64.8219 ± 0.3429	
1-K	65.5704 ± 0.2724	

Velocities at 1 1/2 ft. Away from Exit Plane

(Horizontal Traverse)

Location	Velocity	
1-A	64.7447 ± 0.2819	
3-A	64.8496 ± 0.2901	
5-A	64.9288 ± 0.3251	
7-A	65.0221 ± 0.3160	
9-A	65.0588 ± 0.2738	
11-A	65.2195 ± 0.2378	(20:1)
15-A	64.7844 ± 0.2583	
17-A	64.9005 ± 0.2737	
19-A	65.0503 ± 0.2985	
21-A	65.2870 ± 0.3521	
23-A	65.4387 ± 0.3996	

(Vertical Traverse)

1-C'	64.8637 ± 0.3624	
1-E'	65.1067 ± 0.3340	
1-G'	65.0672 ± 0.2584	
1-I'	64.9062 ± 0.2986	
1-K'	65.3826 ± 0.3707	(20:1)
1-C	64.6425 ± 0.2988	
1-E	64.9373 ± 0.2659	
1-G	64.8212 ± 0.4519	
1-I	65.5481 ± 0.2516	
1-K	65.5425 ± 0.2448	

XI. APPENDIX

A. Sample Calculations

$$\bar{X} = \frac{1}{N}\sum_{i=1}^{n} X_i = \frac{1}{N}\sum_{i=1}^{n}(\text{ZERO} - X_i) = 1.1207$$

$$\sigma = \left[\sum_{i=1}^{n} \frac{(X_i - \bar{X})^2}{n-1}\right] = 1.168 \times 10^{-3}$$

Mean and Standard Deviation Calculated For Point (1-A) After Tunnel Was Raised 2 3/4 in.

Sample Calculation For Velocity:

$$V = \sqrt{2g h_{AIR}} = \sqrt{\frac{2g h_{MAN} \rho_{MAN}}{\rho_{AIR}}}$$

Where $\rho_{AIR} = \frac{P_{AIR}}{R T_{AIR}}$

$$\therefore V = \sqrt{\frac{2g h_{MAN} R T_{AIR} \rho_{MAN}}{P_{AIR}}}$$

To Correct Value To Standard Day ($530^{\circ}R$ - 14.7 psia)

$$V = \sqrt{\frac{2gR\,T_o}{P_o}} \cdot \sqrt{\frac{h_{MAN} T_{AIR} P_o \rho_{MAN}}{T_o P_{AIR}}}$$

Dimensional Check

$$V = \sqrt{\frac{ft}{SEC^2}\left(\frac{Lbf - ft}{Lbm - {}^{\circ}R}\right)\frac{{}^{\circ}R\ ft^2}{Lbf}} \cdot \sqrt{\frac{ft - {}^{\circ}R\ Lbf - ft^2\ Lbm}{ft^2 - Lbf\ ft^3}}$$

$$V = \sqrt{ft^2/SEC^2} = ft/SEC = 63.8\ ft/SEC \quad \text{(BY SLIDERULE)}$$

B. Computer Program for Calculating Mean and Standard Deviation

```
5 PROGRAM DOV
10 DIMENSION X(12),Y(12)
15 READ,(Y(K),K=1,10)
16 INPUT,BASE
25 N=10
26 XN=N
27 DO 28 I=1,10
28 X(I)=BASE-Y(I)
30 SUM=0.0
35 SUM1=0.0
40 DO 45 I=1,N
45 SUM=SUM+X(I)
50 XBAR=SUM/XN
55 DO 65 J=1,N
60 P=(ABS(X(J)-XBAR))**2.
65 SUM1=SUM1+P
66 XN=N
70 SX=SUM1/(XN-1.)
75 SIGMA=SQRT(SX)
80 FORMAT(1X,//*STANDARD DEVIATION=*,F10.4,10X*MEAN=*,F10.4)
81 PRINT 80,SIGMA,XBAR
85 END
90 ENDPROG
95 .4946,.4831,.4870,.4860,.4878,.4826,.4823
100 .4890,.4877,.4843
```

B. Computer Program for Calculating Mean and Standard Deviation

```
5 PROGRAM DON
10 DIMENSION X(12),Y(12)
15 READ,(Y(K),K=1,10)
16 INPUT,BASE
25 N=10
26 XN=N
27 DO 28 I=1,10
28 Y(I)=BASE-Y(I)
30 SUM=0.0
35 SUM1=0.0
40 DO 45 I=1,N
45 SUM=SUM+X(I)
50 XBAR=SUM/XN
55 DO 65 J=1,N
60 P=(ABS(Y(J)-XBAR))**2.
65 SUM1=SUM1+P
66 XN=N
70 SX=SUM1/(XN-1.)
75 SIGMA=SQRT(SX)
80 FORMAT(1X,//*STANDARD DEVIATION=*,F10.4,10X*MEAN=*,F10.4)
81 PRINT 80,SIGMA,XBAR
85 END
90 ENDPROG
95 .4846,.4831,.4870,.4860,.4878,.4826,.4823
100 .4890,.4877,.4843
```

D. Initial Experimental Data

Taken at exit plane - traverse of horizontal center line

See Fig. 5 for location of test points.

Average Butyl Alcohol Temperature - 63.5°F

Corrected Barometric Pressure - 30.005 in. Hg.

Average Air Stream Temperature - 68.5°F

Zero Manometer Reading - 1.5200 in. But. Al.

Location	Readings	Location	Readings
	0.3956		0.3874
1-A	0.3917	3-A	0.3882
	0.3914		0.3881
$\bar{x}$ = 1.1294	0.3903	$\bar{x}$ = 1.1330	0.3863
σ = 0.0020	0.3894	σ = 0.0012	0.3863
	0.3901		0.3862
$\bar{x}$ = 1.1294 $\pm$ 0.0040	0.3896	$\bar{x}$ = 1.1330 $\pm$ 0.0024	0.3852
(20:1) Odds	0.3890	(20:1) Odds	0.3880
	0.3892		0.3856
	0.3898		0.3885
	0.3782		0.3712
5-A	0.3778	7-A	0.3690
	0.3778		0.3698
$\bar{x}$ = 1.1420	0.3786	$\bar{x}$ = 1.1502	0.3703
σ = 0.0012	0.3773	σ = 0.0013	0.3704
	0.3753		0.3700
$\bar{x}$ = 1.1420 $\pm$ 0.0024	0.3775	$\bar{x}$ = 1.1502 $\pm$ 0.0026	0.3693
(20:1) Odds	0.3800	(20:1) Odds	0.3693
	0.3786		0.3670
	0.3784		0.3715

Location	Readings	Location	Readings
	0.3623		0.3660
9-A	0.3627	11-A	0.3641
	0.3635		0.3660
$\bar{x}$ = 1.1567	0.3630	$\bar{x}$ = 1.1547	0.3637
σ = 0.0011	0.3620	σ = 0.0018	0.3637
	0.3620		0.3687
$\bar{x}$ = 1.1567 $\pm$ 0.0022	0.3637	$\bar{x}$ = 1.1547 $\pm$ 0.0036	0.3630
(20:1) Odds	0.3641	(20:1) Odds	0.3646
	0.3650		0.3661
	0.3645		0.3674
	0.3874		0.3832
15-A	0.3910	17-A	0.3855
	0.3910		0.3846
$\bar{x}$ = 1.1298	0.3900	$\bar{x}$ = 1.1355	0.3832
σ = 0.0017	0.3925	σ = 0.0013	0.3850
	0.3925		0.3824
$\bar{x}$ = 1.1298 $\pm$ 0.0034	0.3905	$\bar{x}$ = 1.1355 $\pm$ 0.0026	0.3853
(20:1) Odds	0.3877	(20:1) Odds	0.3843
	0.3897		0.3867
	0.3893		0.3844

Location	Readings	Location	Readings
	0.3795		0.3682
19-A	0.3764	21-A	0.3714
	0.3762		0.3690
$\bar{x}$ = 1.1431	0.3762	$\bar{x}$ = 1.1500	0.3723
σ = 0.0013	0.3765	σ = 0.0020	0.3723
	0.3765		0.3726
$\bar{x}$ = 1.1431 $\pm$ 0.0026	0.3781	$\bar{x}$ = 1.1500 $\pm$ 0.0040	0.3691
(20:1) Odds	0.3766	(20:1) Odds	0.3693
	0.3777		0.3694
	0.3750		0.3666

	0.3595
23-A	0.3656
	0.3656
$\bar{x}$ = 1.1546	0.3656
σ = 0.0027	0.3693
	0.3636
$\bar{x}$ = 1.1546 $\pm$ 0.0054	0.3675
(20:1) Odds	0.3637
	0.3672
	0.3662

Average Butyl Alcohol Reservoir Temperature - 70°F

Corrected Barometric Pressure - 31.46 in. Hg.

Average Air Stream Temperature - 74°F

Zero Manometer Reading - 1.6027 in. But. Al.

Location	Readings	Location	Readings
	0.4495		0.4508
1-C'	0.4485	1-E'	0.4521
	0.4456		0.4510
$\bar{x}$ = 1.1551	0.4503	$\bar{x}$ = 1.1514	0.4513
σ = 0.0017	0.4490	σ = 0.0009	0.4507
	0.4470		0.4496
$\bar{x}$ = 1.1551 $\pm$ 0.0034	0.4452	$\bar{x}$ = 1.1514 $\pm$ 0.0018	0.4510
(20:1) Odds	0.4472	(20:1) Odds	0.4524
	0.4472		0.4524
	0.4465		0.4513
	0.4454		0.4447
1-G'	0.4432	1-I'	0.4455
	0.4393		0.4460
$\bar{x}$ = 1.1606	0.4422	$\bar{x}$ = 1.1558	0.4460
σ = 0.0034	0.4405	σ = 0.0016	0.4452
	0.4402		0.4478
$\bar{x}$ = 1.1606 $\pm$ 0.0068	0.4415	$\bar{x}$ = 1.1558 $\pm$ 0.0032	0.4478
(20:1) Odds	0.4417	(20:1) Odds	0.4478
	0.4373		0.4490
	0.4496		0.4490

Location	Readings	Location	Readings
	0.4345		0.4694
1-K·	0.4325	1-C	0.4675
	0.4331		0.4641
$\bar{x}$ = 1.1722	0.4330	$\bar{x}$ = 1.1368	0.4672
σ = 0.0025	0.4291	σ = 0.0019	0.4658
	0.4291		0.4658
$\bar{x}$ = 1.1722 ± 0.0050	0.4275	$\bar{x}$ = 1.1368 ± 0.0038	0.4660
(20:1) Odds	0.4284	(20:1) Odds	0.4655
	0.4284		0.4627
	0.4295		0.4647
	0.4688		0.4642
1-E	0.4711	1-G	0.4642
	0.4685		0.4644
$\bar{x}$ = 1.1322	0.4712	$\bar{x}$ = 1.1389	0.4647
σ = 0.0013	0.4706	σ = 0.0019	0.4615
	0.4690		0.4657
$\bar{x}$ = 1.1322 ± 0.0026	0.4722	$\bar{x}$ = 1.1389 ± 0.0038	0.4610
(20:1) Odds	0.4712	(20:1) Odds	0.4612
	0.4712		0.4663
	0.4712		0.4651

Location	Readings	Location	Readings
	0.4396		0.4408
1-I	0.4381	1-K	0.4412
	0.4414		0.4422
$\bar{x}$ = 1.1631	0.4414	$\bar{x}$ = 1.1597	0.4422
σ = 0.0021	0.4393	σ = 0.0027	0.4450
	0.4397		0.4432
$\bar{x}$ = 1.1631 $\pm$ 0.0042	0.4350	$\bar{x}$ = 1.1597 $\pm$ 0.0054	0.4481
(20:1) Odds	0.4415	(20:1) Odds	0.4390
	0.4415		0.4462
	0.4380		0.4420

Data taken at 1 1/2 ft. from exit plane

Average Butyl Alcohol Temperature - 66°F

Corrected Barometric Pressure - 29.41 in. Hg.

Average Air Stream Temperature - 66°F

Zero Manometer Reading - 1.6180 in. But. Al.

Location	Readings	Location	Readings
	0.4795		0.4710
1-A	0.4765	3-A	0.4720
	0.4730		0.4720
$\bar{x}$ = 1.1413	0.4757	$\bar{x}$ = 1.1450	0.4700
σ = 0.0018	0.4776	σ = 0.0019	0.4731
	0.4777		0.4763
$\bar{x}$ = 1.1413 ± 0.0036	0.4753	$\bar{x}$ = 1.1450 ± 0.0038	0.4720
(20:1) Odds	0.4762	(20:1) Odds	0.4738
	0.4787		0.4749
	0.4766		0.4744
	0.4757		0.4690
5-A	0.4706	7-A	0.4660
	0.4680		0.4664
$\bar{x}$ = 1.1478	0.4714	$\bar{x}$ = 1.1511	0.4664
σ = 0.0023	0.4694	σ = 0.0022	0.4650
	0.4694		0.4665
$\bar{x}$ = 1.1478 ± 0.0046	0.4705	$\bar{x}$ = 1.1511 ± 0.0044	0.4637
(20:1) Odds	0.4680	(20:1) Odds	0.4700
	0.4682		0.4655
	0.4710		0.4704

Location	Readings	Location	Readings
	0.4687		0.4607
9-A	0.4645	11-A	0.4597
	0.4645		0.4590
$\bar{x}$ = 1.1524	0.4654	$\bar{x}$ = 1.1581	0.4607
σ = 0.0017	0.4685	σ = 0.0012	0.4601
	0.4651		0.4582
$\bar{x}$ = 1.1524 $\pm$ 0.0034	0.4650	$\bar{x}$ = 1.1581 $\pm$ 0.0024	0.4604
(20:1) Odds	0.4657	(20:1) Odds	0.4604
	0.4655		0.4580
	0.4634		0.4618
	0.4731		0.4703
15-A	0.4744	17-A	0.4703
	0.4764		0.4723
$\bar{x}$ = 1.1427	0.4761	$\bar{x}$ = 1.1468	0.4723
σ = 0.0015	0.4771	σ = 0.0017	0.4704
	0.4775		0.4721
$\bar{x}$ = 1.1427 $\pm$ 0.0030	0.4746	$\bar{x}$ = 1.1468 $\pm$ 0.0034	0.4692
(20:1) Odds	0.4760	(20:1) Odds	0.4692
	0.4739		0.4712
	0.4740		0.4747

Location	Readings	Location	Readings
	0.4675		0.4632
19-A	0.4675	21-A	0.4603
	0.4661		0.4566
$\bar{x}$ = 1.1521	0.4670	$\bar{x}$ = 1.1605	0.4570
σ = 0.0020	0.4656	σ = 0.0026	0.4550
	0.4632		0.4585
$\bar{x}$ = 1.1521 $\pm$ 0.0040	0.4665	$\bar{x}$ = 1.1605 $\pm$ 0.0052	0.4554
(20:1) Odds	0.4692	(20:1) Odds	0.4580
	0.4634		0.4558
	0.4634		0.4552

	0.4584
23-A	0.4506
	0.4520
$\bar{x}$ = 1.1659	0.4500
σ = 0.0031	0.4512
	0.4516
$\bar{x}$ = 1.1659 $\pm$ 0.0062	0.4486
(20:1) Odds	0.4541
	0.4553
	0.4488

Location	Readings	Location	Readings
	0.4787		0.4706
1-C	0.4810	1-E	0.4665
	0.4790		0.4704
$\bar{x}$ = 1.1377	0.4775	$\bar{x}$ = 1.1481	0.4724
σ = 0.0020	0.4792	σ = 0.0016	0.4713
	0.4830		0.4701
$\bar{x}$ = 1.1377 $\pm$ 0.0040	0.4785	$\bar{x}$ = 1.1481 $\pm$ 0.0032	0.4690
(20:1) Odds	0.4834	(20:1) Odds	0.4690
	0.4815		0.4703
	0.4811		0.4694
	0.4812		0.4490
1-G	0.4725	1-I	0.4476
	0.4724		0.4510
$\bar{x}$ = 1.1440	0.4780	$\bar{x}$ = 1.1698	0.4495
σ = 0.0036	0.4756	σ = 0.0014	0.4463
	0.4704		0.4473
$\bar{x}$ = 1.1440 $\pm$ 0.0072	0.4716	$\bar{x}$ = 1.1698 $\pm$ 0.0028	0.4482
(20:1) Odds	0.4716	(20:1) Odds	0.4485
	0.4765		0.4484
	0.4704		0.4464

Location	Readings	Location	Readings
	0.4486		0.4743
1-K	0.4493	1-C'	0.4743
	0.4470		0.4730
$\bar{x}$ = 1.1696	0.4460	$\bar{x}$ = 1.1455	0.4700
σ = 0.0013	0.4482	σ = 0.0027	0.4758
	0.4484		0.4744
$\bar{x}$ = 1.1696 $\pm$ 0.0026	0.4482	$\bar{x}$ = 1.1455 $\pm$ 0.0054	0.4750
(20:1) Odds	0.4494	(20:1) Odds	0.4697
	0.4506		0.4690
	0.4483		0.4694
	0.4626		0.4675
1-E'	0.4664	1-G'	0.4633
	0.4655		0.4654
$\bar{x}$ = 1.1541	0.4623	$\bar{x}$ = 1.1527	0.4656
σ = 0.0024	0.4664	σ = 0.0015	0.4670
	0.4650		0.4640
$\bar{x}$ = 1.1541 $\pm$ 0.0048	0.4669	$\bar{x}$ = 1.1527 $\pm$ 0.0030	0.4650
(20:1) Odds	0.4626	(20:1) Odds	0.4650
	0.4611		0.4634
	0.4605		0.4667

Location	Readings	Location	Readings
	0.4733		0.4520
1-I'	0.4704	1-K'	0.4552
	0.4724		0.4577
$\bar{x}$ = 1.1470	0.4700	$\bar{x}$ = 1.1639	0.4510
σ = 0.0020	0.4753	σ = 0.0028	0.4582
	0.4695		0.4541
$\bar{x}$ = 1.1470 $\pm$ 0.0040	0.4704	$\bar{x}$ = 1.1639 $\pm$ 0.0056	0.4567
(20:1) Odds	0.4694	(20:1) Odds	0.4536
	0.4694		0.4510
	0.4700		0.4510

Rerun of exit plane after elevating tunnel 2 1/4 in.

Average Butyl Alcohol Temperature - 58°F

Corrected Barometric Pressure - 29.72 in. Hg.

Average Air Stream Temperature - 73°F

Zero Manometer Reading - 1.6085 in. But. Al.

Location	Readings	Location	Readings
	0.4871		0.4846
1-A	0.4876	3-A	0.4831
	0.4873		0.4870
$\bar{x}$ = 1.1207	0.4891	$\bar{x}$ = 1.1231	0.4860
σ = 0.0012	0.4871	σ = 0.0024	0.4878
	0.4892		0.4826
$\bar{x}$ = 1.1207 $\pm$ 0.0024	0.4880	$\bar{x}$ = 1.1231 $\pm$ 0.0048	0.4823
(20:1) Odds	0.4872	(20:1) Odds	0.4890
	0.4857		0.4877
	0.4894		0.4843
	0.4770		0.4771
5-A	0.4741	7-A	0.4804
	0.4801		0.4772
$\bar{x}$ = 1.1309	0.4745	$\bar{x}$ = 1.1299	0.4817
σ = 0.0020	0.4795	σ = 0.0023	0.4796
	0.4776		0.4817
$\bar{x}$ = 1.1309 $\pm$ 0.0040	0.4782	$\bar{x}$ = 1.1299 $\pm$ 0.0046	0.4771
(20:1) Odds	0.4775	(20:1) Odds	0.4795
	0.4791		0.4760
	0.4785		0.4757

Location	Readings	Location	Readings
	0.4696		0.4558
9-A	0.4650	11-A	0.4565
	0.4681		0.4560
$\bar{x}$ = 1.1425	0.4662	$\bar{x}$ = 1.1528	0.4540
σ = 0.0022	0.4646	σ = 0.0015	0.4531
	0.4640		0.4558
$\bar{x}$ = 1.1425 $\pm$ 0.0044	0.4640	$\bar{x}$ = 1.1528 $\pm$ 0.0030	0.4587
(20:1) Odds	0.4683	(20:1) Odds	0.4567
	0.4670		0.4552
	0.4632		0.4550
	0.4977		0.4895
15-A	0.4955	17-A	0.4896
	0.4965		0.4900
$\bar{x}$ = 1.1124	0.4933	$\bar{x}$ = 1.1184	0.4871
σ = 0.0014	0.4963	σ = 0.0023	0.4871
	0.4942		0.4900
$\bar{x}$ = 1.1124 $\pm$ 0.0028	0.4973	$\bar{x}$ = 1.1184 $\pm$ 0.0046	0.4924
(20:1) Odds	0.4963	(20:1) Odds	0.4924
	0.4963		0.4941
	0.4975		0.4884

Location	Readings	Location	Readings
	0.4798		0.4627
19-A	0.4767	21-A	0.4690
	0.4764		0.4693
$\bar{x}$ = 1.1301	0.4808	$\bar{x}$ = 1.1404	0.4684
σ = 0.0016	0.4802	σ = 0.0009	0.4674
	0.4771		0.4679
$\bar{x}$ = 1.1301 $\pm$ 0.0032	0.4771	$\bar{x}$ = 1.1404 $\pm$ 0.0018	0.4691
(20:1) Odds	0.4793	(20:1) Odds	0.4674
	0.4784		0.4675
	0.4784		0.4666

	0.4508
23-A	0.4527
	0.4542
$\bar{x}$ = 1.1511	0.4582
σ = 0.0039	0.4550
	0.4600
$\bar{x}$ = 1.1511 $\pm$ 0.0078	0.4622
(20:1) Odds	0.4616
	0.4600
	0.4592

Location	Readings	Location	Readings
	0.5000		0.4807
1-C	0.5046	1-E	0.4830
	0.5010		0.4826
$\bar{x}$ = 1.1113	0.4975	$\bar{x}$ = 1.1275	0.4846
σ = 0.0036	0.4944	σ = 0.0026	0.4800
	0.4954		0.4807
$\bar{x}$ = 1.1113 $\pm$ 0.0072	0.4954	$\bar{x}$ = 1.1275 $\pm$ 0.0052	0.4815
(20:1) Odds	0.4956	(20:1) Odds	0.4783
	0.4925		0.4756
	0.4954		0.4830
	0.4736		0.4444
1-G	0.4775	1-I	0.4400
	0.4804		0.4407
$\bar{x}$ = 1.1327	0.4763	$\bar{x}$ = 1.1671	0.4407
σ = 0.0025	0.4788	σ = 0.0013	0.4414
	0.4756		0.4405
$\bar{x}$ = 1.1327 $\pm$ 0.0050	0.4750	$\bar{x}$ = 1.1671 $\pm$ 0.0026	0.4405
(20:1) Odds	0.4744	(20:1) Odds	0.4416
	0.4731		0.4415
	0.4730		0.4427

Location	Readings	Location	Readings
	0.4406		0.4788
1-K	0.4406	1-C'	0.4781
	0.4386		0.4800
$\bar{x}$ = 1.1675	0.4430	$\bar{x}$ = 1.1303	0.4763
σ = 0.0012	0.4420	σ = 0.0021	0.4763
	0.4413		0.4793
$\bar{x}$ = 1.1675 $\pm$ 0.0024	0.4413	$\bar{x}$ = 1.1303 $\pm$ 0.0042	0.4800
(20:1) Odds	0.4400	(20:1) Odds	0.4747
	0.4422		0.4814
	0.4406		0.4771
	0.4723		0.4712
1-E'	0.4725	1-G'	0.4710
	0.4751		0.4710
$\bar{x}$ = 1.1376	0.4718	$\bar{x}$ = 1.1415	0.4722
σ = 0.0024	0.4685	σ = 0.0041	0.4643
	0.4687		0.4620
$\bar{x}$ = 1.1376 $\pm$ 0.0048	0.4727	$\bar{x}$ = 1.1415 $\pm$ 0.0082	0.4621
(20:1) Odds	0.4695	(20:1) Odds	0.4674
	0.4710		0.4654
	0.4674		0.4630

Location	Readings	Location	Readings
	0.4699		0.4407
1-I'	0.4627	1-K'	0.4430
	0.4670		0.4439
$\bar{x}$ = 1.1409	0.4670	$\bar{x}$ = 1.1674	0.4425
σ = 0.0025	0.4724	σ = 0.0017	0.4415
	0.4684		0.4397
$\bar{x}$ = 1.1409 $\pm$ 0.0050	0.4667	$\bar{x}$ = 1.1674 $\pm$ 0.0034	0.4403
(20:1) Odds	0.4684	(20:1) Odds	0.4384
	0.4675		0.4396
	0.4664		0.4412

UNCLASSIFIED

Security Classification

DOCUMENT CONTROL DATA - R & D

Security classification of title, body of abstract and indexing annotation must be entered when the overall report is classified

ORIGINATING ACTIVITY (Corporate author)

School of Engineering
University of Massachusetts
Amherst, Massachusetts 01002

2a. REPORT SECURITY CLASSIFICATION

UNCLASSIFIED

2b. GROUP

REPORT TITLE

DEFINING THE FLOW FIELD OF AN OPEN-JET WIND TUNNEL

DESCRIPTIVE NOTES (Type of report and inclusive dates)

AUTHOR(S) (First name, middle initial, last name)

Donald B. Poole and Duane E. Cromack

REPORT DATE	7a. TOTAL NO. OF PAGES	7b. NO. OF REFS
June 1970	83	7

CONTRACT OR GRANT NO	9a. ORIGINATOR'S REPORT NUMBER(S)
ONR-N00014-68-A-0146	THEMIS-UM-70-3
b. PROJECT NO In-house Project Number N00014-68-A-0146-12	9b. OTHER REPORT NO(S) (Any other numbers that may be assigned this report)

DISTRIBUTION STATEMENT

Distribution of this document is unlimited.

11. SUPPLEMENTARY NOTES	12. SPONSORING MILITARY ACTIVITY
	Department of Defense (Project THEMIS)

13. ABSTRACT

This investigation deals with mapping the velocities at successive cross-sectional planes in the test section of an open-jet wind tunnel. The instrumentation was chosen so that the total uncertainty on the calculated velocity would be less than 1% with a 95% confidence level.

The jet was studied using photography and a grid-and-tuft scheme, and it was determined that the same flow characteristics appear at both high and low flow rates.

The best probable location for model testing was determined to be 1-1/4 ft. to 2-1/2 ft. away from the exit plane of the tunnel as indicated by the combined pressure measurements and the photographic studies. It was also noted that turbulent mixing occurred between the jet and the still air in the room. The turbulence had a tendency to move in toward the center of the jet at successive planes from the exit plane of the tunnel. The most drastic change in turbulent mixing occurred at a cross-section 3 ft. away from the exit plane. Recommendations for alterations to the facility are made for testing at or near the 3 ft. location.

DD FORM 1 NOV 65 1473 (PAGE 1)

S/N 0101-807-6811

UNCLASSIFIED

Security Classification

A-31140

KEY WORDS	LINK A		LINK B		LINK C	
	ROLE	WT	ROLE	WT	ROLE	WT
Wind Tunnel						
Open-Jet Wind Tunnel						
Velocity Field						